1-1-2019

Analytical Modeling And Life Cycle Assessment Of A Solar Powered Vapor Absorption Cooling System

Harold A. Walters

ANALYTICAL MODELING AND LIFE CYCLE ASSESSMENT OF A SOLAR POWERED VAPOR ABSORPTION COOLING SYSTEM

A Thesis
presented in partial fulfillment of requirements
for the degree of Master of Science
in the Department of Mechanical Engineering
The University of Mississippi

by

Harold A. Walters

December 2019

ABSTRACT

Vapor absorption cooling systems (VACS) offer an environmentally friendly alternative to the standard vapor compression cooling systems (VCCS) for cooling homes, businesses, factories, and other buildings. VACS use low-grade thermal energy to achieve a cooling effect and require minimal electrical input for the liquid solution pump used for circulation within the system. The thermal energy which powers these systems can be provided through several means; one popular form is through the use of solar thermal collectors. This paper provides a process for determining the overall size and configuration of the VACS depending upon the operating conditions of selected components. A mathematical model is provided for the sizing for a 100 refrigeration-ton (RT) VACS. The thermal network which powers the system is composed of counter flow heat exchangers, hot water storage tanks, flat-plate solar thermal collectors, auxiliary electric heaters, and liquid pumps. A life cycle assessment of the sized mathematical model is then presented, with a comparison to the life cycles of heating the system using only electric heaters powered by electricity produced by coal power stations and wood pellet power stations. The global warming potential of each heat source is compared to determine the most environmentally friendly solution and environmental payback period.

The proposed solar thermal system for the 100 RT VACS calls for the implementation of 920 flat-plate solar collectors, in arrays consisting of 10 parallel branches of 23 collectors in series, with 4 hot water tanks, and 8 heat exchangers. It is seen that by using the proposed solar thermal system subsidized by wood pellet powered auxiliary heaters, the CO_2 emissions of the

system are 10 times less than that produced using coal power. The solar and wood pellet co-powered system would replace the usage of almost 1750 metric tons of coal per year. The solar thermal system repays the energy consumed and CO_2 produced during the manufacturing stage within 1.9 and 0.2 years respectively.

LIST OF ABBREVIATIONS AND SYMBOLS

Nomenclature		*Subscripts*	
A_C	Area of Solar Collector	a	Absorber
COP	Coefficient of Performance	amb	Ambient
C_p	Specific Heat	aux	Auxiliary
C^*	Capacitance Ratio	c	Condenser
F_R	Heat Removal Factor	cold	Cold Side Flow
h	Enthalpy	e	Evaporator
Δh_{mix}	Enthalpy of Mixing	g	Generator
H_2O	Water	hot	Hot Side Flow
I_T	Solar Irradiation	HX	Heat Exchanger
kg CO_2-eq	kg of CO_2 equivalent pollutant	i, o	in, out
LiBr	Lithium Bromide	L	Lithium Bromide
m	Mass of Water	Liq.	Liquid
$\dot{m}$	Mass Flowrate	load	Required by Generator
NH_3	Ammonia	max	Maximum
NTU	Number of Thermal Units	min	Minimum
P	Pressure	n, j	Number of Branches
$\dot{Q}$	Heat Transfer Rate	P	Pump
T	Temperature	req.	Required
t	Time	s	Hot Water Tank
T_s^+	New Temperature	sc	Solar Collector
STS	Solar Thermal System	sca	Solar Collector Array
UA	Overall Heat Transfer Coefficient – Area Product	Sat. L	Saturated Liquid
U_L	Overall Conductance	Sat. V	Saturated Vapor
VACS	Vapor Absorption Cooling System	S.H.V.	Superheated Vapor
VCCS	Vapor Compression Cooling System	ss	Strong Solution
$\dot{W}$	Work Rate	u	Useful
α	Absorptivity	W	Water
ε	Effectiveness of Heat Exchanger	ws	Weak Solution
ξ	Concentration of Lithium Bromide by Mass	2-Phase	Liquid-Vapor Mixture
λ	Circulation Ratio		
η_{exergy}	Exergetic Coefficient of Performance		
τ	Transmissivity		
χ	Mole Fraction		

ACKNOWLEDGEMENTS

I would like to thank my thesis adviser, Dr. Tejas Pandya, my committee members, Dr. Tyrus McCarty and Dr. Yeom Taiho, as well as the rest of the University of Mississippi Mechanical Engineering staff for guiding and challenging me in my academic career as well as providing me with support and wisdom. I could not have financed my studies without the assistantship provided by the Department of Mechanical Engineering.

In addition, I thank my family and friends for providing encouragement and having faith in me.

TABLE OF CONTENTS

LIST OF TABLES

LIST OF FIGURES

CHAPTER 1: INTRODUCTION

Cooling is a major concern to both residential and industrial markets worldwide [1], with 15% of all electricity produced in 2017 being consumed solely for the purpose of air conditioning [2]. Currently the cooling market is dominated by vapor compression cooling systems (VCCS) [3] which utilize mechanical compressors that consume large amounts of electricity [4]. The operation of these systems has not evolved since the birth of the technology by Willis Carrier in 1926 [5]. With approximately 80% of the world's electricity being produced by the combustion of fossil fuels [2], which release greenhouse gasses into the atmosphere [1], the environmental impacts stemming from the use of VCCS are large and will increase with the projected growth in cooling systems worldwide [6, 7]. Between 1990 and 2016 the number of cooling systems worldwide tripled to 1.6 billion units; which consumed over 2000 Terawatt-hours of electricity and produced 1130 million metric tons of CO_2 in 2016 alone [6]. The increase in global electricity demand grew from 14% in 2016 [6] to 15% in 2017 [1] agrees with projected trends of increasing demand [6]. Due to population growth, urbanization, and rising income levels the usage of air conditioning units is predicted to soar to 4.5 billion by 2050, which will have a staggering power demand [5, 8]. India is expected to host the largest market for cooling systems, increasing from 14 million units to nearly 1 billion [5]. As the usage of air conditioning systems increases, so do temperatures as the global warming effects of manufacturing and powering the cooling systems increase; creating a vicious cycle [8].

In 2018, over half of all cooling systems were located in the United States and China [6]. In 2015 87% of U.S. homes used cooling systems [9], where the majority of southern states tend to operate central cooling systems all summer long [10]. In addition to the production of CO_2 that powering these systems requires, the refrigerants used by VCCS's are harmful to the environment [3, 4]. The refrigerants release chlorofluorocarbons and hydrofluorocarbons into the atmosphere, which contribute to the greenhouse effect [4, 6, 11], thus increasing the future demand for cooling [6].

Vapor absorption cooling systems (VACS) provide an environmentally friendly alternative to the VCCS. VACS use a thermal compression system, which is primarily powered by low-grade thermal energy and uses VACS use ecofriendly sorbent-refrigerant pairs [1-4, 7, 12-25]. The most common sorbent-refrigerant pairs are lithium bromide and water ($LiBr-H_2O$) and water and ammonia (H_2O-NH_3) systems, which are typically used for cooling and refrigeration respectively [12]. Thermal energy can be provided to the VACS by means such as solar thermal collectors, biomass, or by waste heat from industrial processes [16]. The use of solar thermal collectors is advantageous because as the temperature and cooling demand rises during summer months, the amount of solar irradiation available to power the VACS also increases.

Several experimental studies have been performed to determine the amount of cooling a given VACS can produce depending on the size, type, location, and configuration of a given solar collector [1, 2, 7, 13-20]. However, there is a lack of literature on the sizing of a solar collector and thermal storage system to deliver a prescribed amount of thermal energy to VACS for the purpose of attaining a desired cooling effect. The size and configuration of the system are dependent upon the operating conditions of the components. Misconceptions of system sizing

and configuration can lead to underperforming or oversized systems. The resources used to produce, manufacture, transport, assemble, use, deconstruct, and dispose of these products impact the environment. Improperly sized systems cause additional and unnecessary impacts. The accounting of the resources and energy consumed to create a product is referred to as a life cycle assessment.

The purpose of this thesis is to discuss the workings and current state of technology for VACS and the related components which compose the thermal network. Then, to develop an analytical approach for determining the size and configuration of the VACS and solar thermal network for a prescribed cooling demand. Then, discuss and perform a life cycle assessment which compares heat energy sources for the VACS.

CHAPTER 2: REVIEW OF VACS AND INTRODUCTION OF SOLAR THERMAL NETWORK

2.1 Vapor Absorption vs Vapor Compression Cooling Systems

Vapor compression and vapor absorption systems function similarly. Aside from the means of compression, the systems utilize the same components; the condenser, expansion valve, and evaporator [3, 12]. Figure 1 and Figure 2 show the system schematics for standard vapor compression cooling systems and a single effect vapor absorption cooling system with heat exchanger. The inclusion of the heat exchanger in Figure 2, although not required for system function, is commonly used for its improvement of system performance [2, 3, 12, 15-21]. The horizontal dashed line in Figure 1 and Figure 2 splits the system into high- and low-pressure sides. The pressures of the high and low side are dependent upon the pressures of the condenser (P_c) and the evaporator (P_e) respectively [12]. In these figures, components to the right of the vertical dashed line in comprise the compression systems; mechanical compressor for VCCS, and thermal compressor for VACS. The thermal compressor is composed of five components; absorber, pump heat exchanger, generator, and expansion valve.

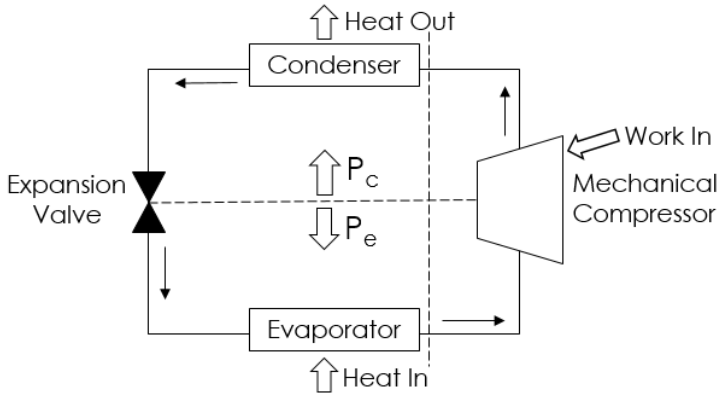

Figure 1: Schematic Diagram of Vapor Compression Cooling System, VCCS

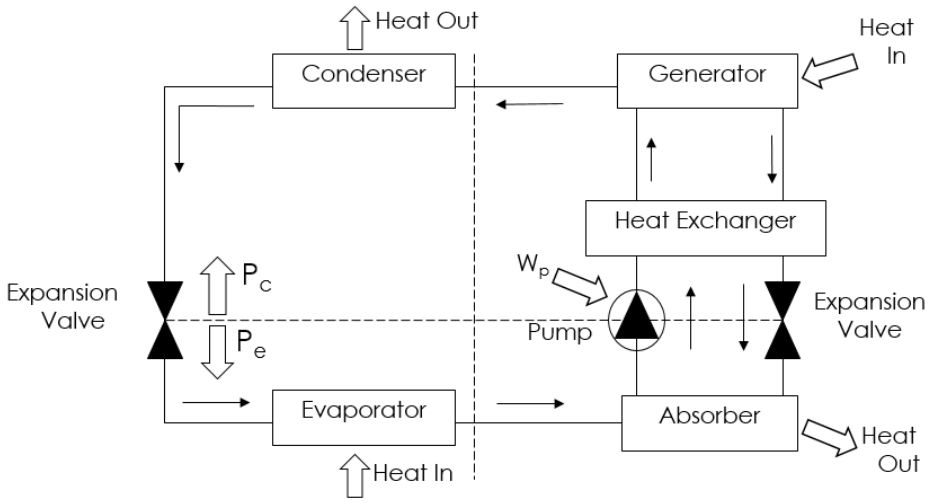

Figure 2: Schematic Diagram of Vapor Absorption Cooling System, VACS

In VCCS, high pressure and high temperature superheated vapor refrigerant enters the condenser to undergo constant pressure heat exhaustion; leaving the refrigerant a cooler, high pressure, saturated liquid. Then the refrigerant undergoes adiabatic throttling through the expansion valve; creating a two-phase, liquid-vapor, refrigerant at low pressure and lower temperature. In the evaporator, the refrigerant undergoes constant pressure heat intake; creating cold, low pressure, saturated vapor refrigerant. Finally, the mechanical compressor compresses

the refrigerant back to a high temperature, high pressure superheated vapor so that it can be recirculated [4].

For the VACS, the condenser, expansion valve, and evaporator perform the same functions as in VCCS [1-4, 7, 12-16, 20, 21]; however, the means of compression are completely different. VACS require the use of a refrigerant and a sorbent pair, called a working pair. As the refrigerant leaves the evaporator as a saturated vapor, it flows into the absorber, which holds the liquid sorbent solution. The vapor refrigerant is absorbed into the liquid sorbent; creating a liquid solution of refrigerant and sorbent. This solution is then pumped to the generator, where sufficient heat is added to induce boiling of the liquid refrigerant. The refrigerant is boiled out of solution to return to the system as a high temperature, high pressure superheated vapor. After the refrigerant is boiled out of the solution, the sorbent flows back into the absorber [2-4, 12, 13, 15 16, 18, 21]. The purpose of the heat exchanger is to preheat the solution for the generator [3, 15-21]. By using the sorbent-refrigerant pair and having the refrigerant absorbed into solution in the absorber, a low power solution pump can be used to circulate the system as opposed to a high-power mechanical compressor [25].

2.2 Working Pairs

A given sorbent-refrigerant pair must exhibit certain characteristics to function properly as a working pair. Some of the ideal key features of these pairing are as follows:

- Refrigerant must be highly soluble in the sorbent [21, 24, 26]
- Large differences in the boiling points of the sorbent and refrigerant [3, 12]
- Heat of mixing should be kept small [12]
- Refrigerant-sorbent solution must have high thermal conductivity and low viscosity [12]
- Working pair does not undergo crystallization [3, 12, 16, 17, 21, 24, 25]
- The mixture should be safe, chemically stable, non-corrosive, inexpensive, and should be easily available [12, 26]

- Refrigerant should have low freezing point [12]
- Low surface tension [22, 26]

Two common working pairs are lithium bromide with water (LiBr-H_2O), and water and ammonia (H_2O-NH_3); as sorbent and refrigerant, respectively [3, 12, 21]. The useful temperature range that a given system can be expected to achieve is constrained by the freezing point of the refrigerant [12]. For this reason, the LiBr-H_2O systems, with water having a freezing point of 0°C, are typically used for air conditioning. On the other hand, ammonia, the refrigerant in the H_2O-NH_3 systems, has a freezing point of approximately -77°C [27], allowing these systems to be used for refrigeration and freezer applications [12]. Neither of these working pairs have all of the ideal characteristics. LiBr-H_2O systems suffer from high heat of mixing [1], being highly corrosive [24], and formation of crystals in solution [3, 21, 24, 25]. High heat of mixing is associated with the high solubility of the water in LiBr, and typically a tradeoff is required between these two requirements [12]. The crystallization issue occurs when the concentration of LiBr in the solution becomes too high [3]. Water and ammonia, H_2O-NH_3, systems require an additional component; the rectifying column. This is because water and ammonia have similar boiling points, allowing for a H_2O-NH_3 mix to leave the generator. The rectifying column functions to remove water vapor from the refrigerant, to achieve a purer ammonia vapor [3]. Due to the similar boiling points of water and ammonia, when the refrigerant is being boiled out of solution, water vapor is also created. A rectification column, placed between the generator and condenser, is required for these systems to remove the water vapor from the water-ammonia vapor mixture; leaving a higher quality ammonia vapor to act as the refrigerant [2, 3, 20].

There are two ways to view the sorbent-refrigerant solution; in terms of the sorbent concentration, or in terms of the refrigerant concentration. If the solution has a higher concentration of sorbent than refrigerant, it can be viewed as strong in sorbent or poor in

refrigerant. If the concentration of refrigerant is higher than that of the sorbent, the solution can be called weak in sorbent or rich in refrigerant. These classifications are sometimes abbreviated as strong or weak when viewing sorbent concentrations, and rich or poor when viewing refrigerant concentrations [3, 14]. To keep consistency throughout this review, the selected nomenclature will use strong and weak solution based on sorbent concentration.

2.3 A Closer Look at a LiBr-H_2O VACS System

In VACS, the LiBr sorbent solution and H_2O refrigerant circulate through the system as shown in Figure 3, below. H_2O moves through the condenser, expansion valve, and evaporator as stated above when explaining the VCCS. As the refrigerant vapor enters the absorber, it is introduced to high concentration liquid sorbent, and is absorbed into solution. The absorption of the refrigerant causes the absorber to maintain a low-pressure environment, thus drawing in more vapor [3]. The amount of refrigerant absorbed by the sorbent relies on the temperature, concentration, surface tension, and mass flowrate of the sorbent in the absorber along with the absorber pressure and vapor-solution interface area [3, 22, 28]. The refrigerant releases heat as it is absorbed and undergoes a phase change to liquid [12, 21]. As the high concentration sorbent takes in the refrigerant, the concentration weakens; thereby reducing the ability of the sorbent to take in more refrigerant. The weak solution, $(LiBr)_{ws}$+ H_2O, is pumped through the heat exchanger and into the generator. Once in the generator, heat is added to the solution and the refrigerant is boiled out of the sorbent. The boiling of the refrigerant produces superheated vapor refrigerant, and decreases the concentration of refrigerant in the solution. The removal of refrigerant from the solution, leaves the solution with a higher sorbent concentration. The higher the concentration of sorbent in the generator, the higher the generator temperature must be to

remove the refrigerant. After the refrigerant is removed from the solution in the generator, the strong solution, $(LiBr)_{ss}$+ H_2O, is pumped back into the absorber for reuse [2-4, 12-15, 21, 28].

Boiling in the generator is typically achieved by running a heating coil through the generator, which has high temperature fluid flowing through it. The heat is transferred to the system by convection and conduction while keeping the fluid in the heating tubes separate from the rest of the system [21]. The hot fluid running through the heating coil can be supplied through various means; including excess heat from thermal systems, solar thermal collectors, or simply by the use of axillary heaters [1, 3, 7, 12, 15-20, 25]. These temperatures can be in excess of 100°C depending on system size, system pressure, and sorbent concentration [3].

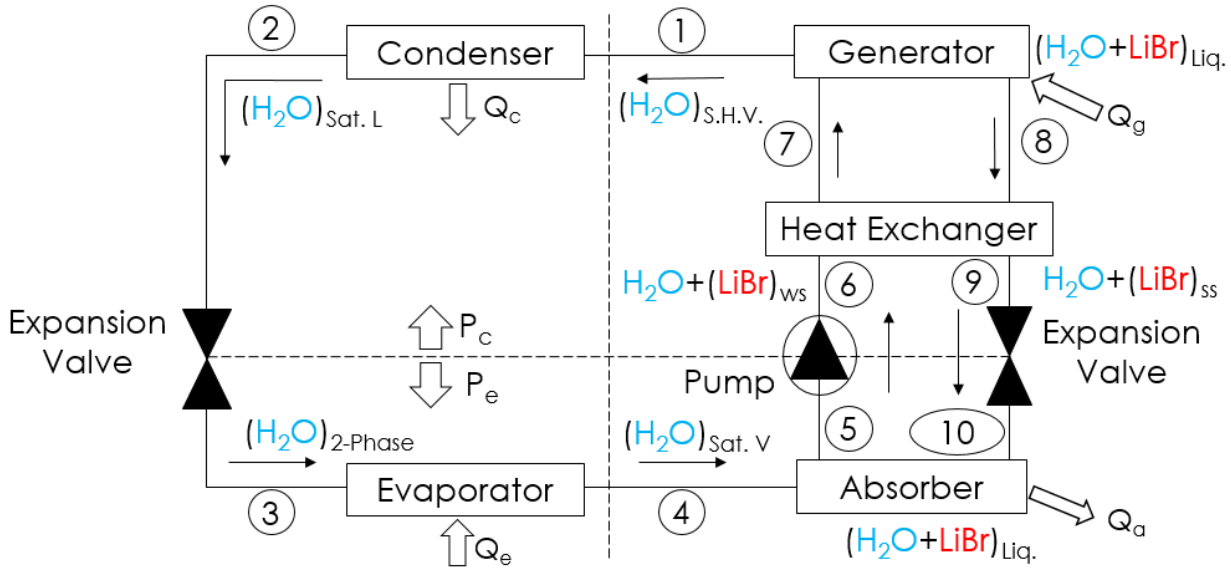

Figure 3: Schematic Diagram of Refrigerant and Sorbent Paths for LiBr- H_2O

The refrigerant and sorbent solution circulate are identified by three characteristics at any point in the system; pressure, temperature, and concentration [1-4, 7, 12-16, 20, 21]. These factors dictate the phase and enthalpy of the components, as well as show if the solution is at risk for crystallization [12, 16, 17, 24, 25]. The equation below shows the calculation for enthalpy of

the mixture. It is determined by examining the concentration of LiBr, ξ, the enthalpy of LiBr and water, h_{LiBr} and h_{H_2O} respectively, and the heat of mixing, Δh_{mix} [12, 21]. The LiBr solution absorbing the water vapor creates an exothermic reaction, resulting in a negative heat of mixtures [12, 21]. Computational methods for calculating the pressure, density, specific heat, enthalpy, and entropy of LiBr-water are provided by [29, 30].

$$h = \xi h_{LiBr} + (1 - \xi) h_{H_2O} + \Delta h_{mix} \quad (1)$$

2.4 Mass and Energy Balance

Under steady state conditions, the mass and energy balance for each component can be summarized as follows, assuming steady state [1-3, 16-18, 20]:

$$\Sigma \dot{m}_i = \Sigma \dot{m}_o \quad (2)$$

$$\Sigma \dot{m}_i x_i = \Sigma \dot{m}_o x_o \quad (3)$$

$$\Sigma \dot{Q} - \Sigma \dot{W} = \Sigma \dot{m}_o h_o - \Sigma \dot{m}_i h_i \quad (4)$$

When these equations are applied to each component, the following equations are determined [1, 2, 13, 15, 16, 21]:

$$\dot{Q}_e = \dot{m}(h_4 - h_3) \quad (5)$$

$$\lambda = \frac{\dot{m}_{ss}}{\dot{m}} = \frac{\xi_{ws}}{\xi_{ss} - \xi_{ws}} \quad (6)$$

$$\dot{m}_{ss} = \lambda \dot{m} \quad (7)$$

$$\dot{m}_{ws} = \dot{m} + \dot{m}_{ss} = (1 + \lambda)\dot{m} \quad (8)$$

$$\dot{Q}_c = \dot{m}(h_1 - h_2) \quad (9)$$

$$\dot{Q}_a = \dot{m}h_4 + \dot{m}_{ss}h_{10} - \dot{m}_{ws}h_5 \quad (10)$$

$$\dot{W}_p = \dot{m}_{ws}\,(h_6 - h_5) \quad (11)$$

$$\dot{Q}_g = \dot{m}\,h_1 + \dot{m}_{ss}h_8 - \dot{m}_{ws}h_7 \quad (12)$$

Where h is enthalpy, Ẇ is power, Q̇ is heat rate, ξ is the mass fraction of LiBr, and χ is mole fraction of LiBr; and subscripts i, o, e, a, c, g, ws, and ss represent in, out, evaporator, absorber, condenser, generator, weak solution, and strong solution with numbers corresponding to state points. The ratio of the mass flowrate of the strong solution, $\dot{m}_{ss}$, to the mass flowrate of refrigerant, ṁ, is referred to as the circulation ratio, λ [2, 12, 13, 16, 21].

Cooling systems are judged primarily by three aspects; the coefficient of performance, the second law efficiency, and the cooling capacity [3, 7, 11, 12, 15, 21]. The coefficient of performance, COP, is defined as the limitation of performance that the system can achieve [4], or the ratio of heat absorbed by the absorber to the rate of heat input to the generator [15]. Typically, the work of the solution pump is ignored [1-4, 7, 12, 14-16, 21, 26]. The second law efficiency, also called the exergetic efficiency, is defined as the maximum work potential that can obtained from an energy system in relation to the surrounding environment. Exergetic efficiency, η_{exergy}, is used to determine the improvement potential of the system [15]. Cooling capacity, or cooling power, is refers to the amount of cooling that the system can offer [3, 12, 15], and thereby is taken to be equivalent to $\dot{Q}_e$ [2, 12]. High COP and exergetic efficiency are desired [1-4, 7, 12-16, 20, 21]. Equations of COP and exergetic efficiency are shown below [12, 21].

$$COP_{VARS} = \frac{\dot{Q}_e}{\dot{Q}_g + \dot{W}_P} \approx \frac{\dot{Q}_e}{\dot{Q}_g} = \frac{T_e}{T_o - T_e}\frac{T_g - T_o}{T_g} \quad (13)$$

$$\eta_{exergy} = \frac{COP}{COP_{max}} = \frac{\dot{Q}_e}{\dot{Q}_g}\frac{T_g}{T_g - T_c}\frac{T_c - T_e}{T_e} \quad (14)$$

VACS have a lower COP compared to VCCS, but due to the VACS system running on thermal energy it is not a fair comparison. The second law efficiency is used to compare different cooling systems, under which the exergetic efficiencies are of the same order [24].

2.5 Review of LiBr-water VACS Experimentation and Improvements

Three main approaches have been used to improve these systems; operational condition improvements, improvements by introducing chemical additives, and design improvements.

2.5.1 Operational Condition Improvements

The operating conditions can change the performance of the system. Generally, increasing the temperature of the generator increases the cooling capacity of the system [7, 15, 19]. However, through experimentation, discrepancies about the impact of increased generator temperature on the COP have arisen. With the increase of generator temperature, the COP has been seen to increase [2, 13, 14], or increase then decrease [14, 17]. The decrease in COP occurs at increasingly higher generator temperatures and can be attributed to additional heat loss of the generator [18] or the increased demand on the heat exchanger [15]. The implementation of a

maximum temperature for the generator should be in place, as to avoid boiling out too much water from solution [19]. This is done to avoid increasing the concentration of LiBr too drastically, resulting in crystallization [19]. The temperature difference between the absorber and generator also have been seen to increase the COP; showing that low absorber temperatures lead to better operation [2, 14, 15]. Increase in generator temperature has also been seen to drive down the exergetic efficiency of the system, meaning that further generator design improvements are needed [15, 18].

The inclusion of a heat exchanger, as well as the effectiveness of the heat exchanger, also impact the system [2, 14, 15]. The purpose of including the heat exchanger is to reduce the energy required by the generator and reduce the heat in the absorber [2, 15]. The heat exchanger functions by having the hot solution leaving the generator preheat the flow entering the generator, and having the cooler flow leaving the absorber cool the flow entering the absorber [2]. Due to this the heat input to the generator is lower, and the heat created in the absorber lower [2, 15]. The effectiveness of the heat exchanger defines the heat transfer rate between the strong and weak solutions [2]. Heat exchangers with higher effectiveness decrease the thermal loads on the system, thereby increasing the COP and exergetic efficiency [2, 15].

2.5.2 Chemical Additives

In an effort to increase the operating range and efficiency of LiBr-water solutions, the addition of chemical surfactants, or additives, has been researched [22, 24-26]. The prime reasons for research in this area is that higher concentrations of sorbent allow for an increase in COP [24], enhancement of heat and mass transfer in the absorber [22, 26], and decrease in

required generator temperature [26]. The addition of surfactants proves to enhance the mixing effects of the solution by decreasing the surface tension [22]. Octanol and 2-thyl-1-hexanol, have been shown to increase the heat transfer effect of the solution, while the addition of n-octanol and 3-octanol corresponds to a higher mass transfer effect [22]. This is because when water vapor is absorbed into the LiBr-solution containing small amounts of alcohol additives, surface turbulence is created; referred to as Marangoni convection [22]. This occurrence is attributed to the change in surface tension around the droplets of surfactant floating on the solution. The turbulence effectively mixes the solution, aiding the transfer process [26]. The addition of sodium formate, NaCOOH, into the LiBr-water system was found to increase the capacity of the solution to absorb water vapor, although the absorption rate was reduced [25, 26]. The introduction of electrically neutral zwitterionic compounds has been shown to increase the maximum concentration of LiBr in solution before crystallization occurs. $N_{222}C_3S$ and $MOR_{1,3}SO_3$ have been shown to allow a significant increase in LiBr concentrations [24].

2.5.3 Design Improvements

One important factor in the design of an absorber is the vapor-solution interface area, which impacts the heat and mass transfer of the absorber [22, 26, 28]. The larger the absorber area is, the higher the efficiency of the absorber [28], which leads to the use of falling film absorbers having dripping, jet-column, and sheet flow types of mass transfer [22]; and the use of bubbling, and sprayer type absorbers [28]. Most absorbers are oversized due to a lack of optimization of interface area. An optimum interface area, based on system parameters, can be found through experimentation [28].

Heat and mass transfer can also be increased by induced oscillation of the solution by means of vibrating the absorber. The introduction of vibration serves to improve the heat transfer coefficient, and decrease the fouling resistance in the tubes. It was seen that the induced vibration successfully increased the mass and heat transfer rates [22].

A method of drastically increasing the COP of the system is to use multiple effect systems [3, 17, 18]. Double effect system use an additional generator and typically a second condenser [3, 16, 17]. By adding these pieces, the COP of the system can almost be doubled, when sufficient temperatures are available [17, 18]. The secondary generator and condenser work at higher temperatures and pressures than the originals [1, 3, 16-18]. There are various schematics for these systems depending on the flow direction; series flow [16-18], parallel flow [17, 18], rear parallel flow, or reverse parallel flow [17]. The COP of the series and parallel systems differ based on operating conditions [16]. The parallel system shows a higher COP for high temperature operations with slow mass flowrates; but as the flowrate increases, the series systems begin to have a higher COP even at lower temperatures [16]. Through an exergy analysis, it can be seen that the generator has the highest irreversibility rate, and therefore is the least efficient component in the cycle [18]. Triple effect systems use a third generator and condenser and have a higher COP than the double effect, but require significantly higher generator temperatures compared to single effect systems [3].

2.6 Flat Plate Solar Thermal Collector

Flat plate collectors are thin rectangular enclosures that allow solar irradiation through the flat transparent front panel (glazing) to heat the absorber plate and fluid running through

pipes attached to the absorber plate, Figure 4. The amount of heat absorbed by a collector depends on the design and use of the collector. The design dictates the number and type of glazings (covers), the aperture area, the temperature and pressure ranges of the collector. A glazing is a flat transparent panel or set of panels facing toward the sun, used to protect the inside of the collector and help capture thermal energy in the enclosure [31]. The angle of inclination to the horizon, the inlet temperature to the collector, and the mass flowrate through the collector depend on use. The availability of solar irradiation changes with time of day, day of the year; while the absorption of solar irradiation changes with the angle of irradiation to the collector [31-35].

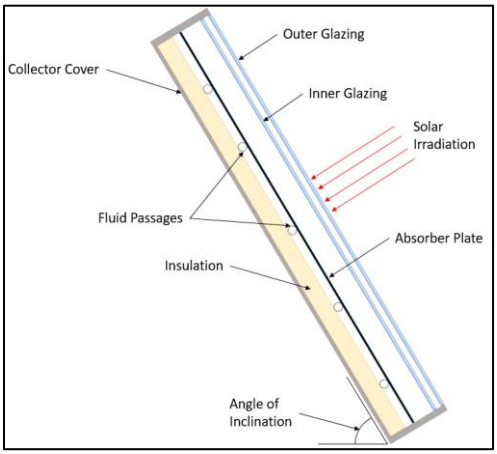

Figure 4: Flat Plate Solar Collector Schematic Diagram

The number and type of glazings used by a flat plate collector change the transmissivity, τ, and absorptivity, α, of the collector. The amount of solar irradiation changes throughout the day and season, as does the ambient temperature. These collectors are mounted at a fixed angle, based on location, to intake the maximum amount solar irradiation, I_T. The collector is typically oriented toward the equator, with an angle of inclination equal to the latitude of the location, which allows for the most irradiation throughout the day [34].

Collector data sheets present terms for efficiency by slope, $F_R U_L$, and intercept, $F_R(\tau\alpha)$, on the collector efficiency plot; where F_R is the collector heat removal factor [31, 36, 37]. The inclusion of the heat removal factor allows for the simplification of the useful heat absorption of the collector to be [31, 36, 37]:

$$\dot{Q}_u = A_c F_R [I_T \tau\alpha - U_L(T_{in} - T_a)] \qquad (15)$$
$$= \dot{m} C_p (T_{out} - T_{in})$$

T_a, T_{in}, and T_{out} are respectively the ambient, inlet, and outlet temperatures; I_T is solar irradiation; and A_c is collector surface area.

2.7 Flat Plate Collector Array

Solar collectors can be connected to one another to increase the output temperature, the mass flowrate out of the array, or both. Collectors arranged in series, Figure 5, have the outlet temperature of one collector used as the inlet temperature for the next collector. This means that the second collector is taking in warmer fluid, which allows for further increase in fluid temperature. The heat absorbed by a series of collectors is equal to the sum of heat collected by each collector in the series; and is calculated as shown below [38]:

$$\dot{Q}_{series} = \dot{Q}_{u,1} + \dot{Q}_{u,2} + \cdots + \dot{Q}_{u,i} \qquad (16)$$
$$= A_{c,1} F_{R,1} \left[I_T (\tau\alpha)_1 - U_{L,1}(T_{in} - T_a) \right]$$
$$+ A_{c,2} F_{R,2} \left[I_T (\tau\alpha)_2 - U_{L,2}\left(T_{in,2} - T_a\right) \right]$$
$$+ \cdots + A_{c,i} F_{R,i} \left[I_T (\tau\alpha)_i - U_{L,i}\left(T_{in,i} - T_a\right) \right]$$

Where each additional $T_{in,i}$ term is the outlet temperature of the previous collector [38]:

$$T_{in,i} = T_{in,i-1} + \frac{\dot{Q}_{u,i-1}}{\dot{m}_{series} C_p} \quad (17)$$

$$T_{out,series} = T_{in,i} + \frac{\dot{Q}_{u,i}}{\dot{m}_{series} C_p} \quad (18)$$

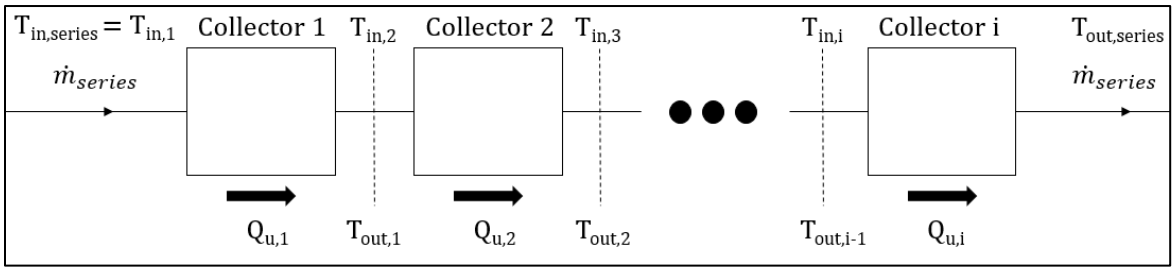

Figure 5: Schematic Diagram of Solar Collectors in Series

Collectors are designed to operate within a given flowrate range. When collectors are placed in parallel, Figure 6, the flows from each branch combine as they leave the collectors and create a higher flowrate, and thereby a higher mass flowrate. By increasing the mass flowrate leaving the collector array, the amount of heat that the array can deliver to the thermal storage system increases [35]. Assuming conservation of mass through each branch of collectors in parallel, the mass flowrate entering and leaving the array is the sum of the mass flowrates from each branch:

$$\dot{m}_{array} = \dot{m}_{branch,1} + \dot{m}_{branch,2} + \cdots + \dot{m}_{branch,j} \quad (19)$$

These arrangements can be combined to absorb a prescribed heat load, assuming constant solar irradiation and ambient temperature [35, 38].

$$\dot{Q}_{array} = \dot{m}_{array} C_p (T_{array,out} - T_{array,in}) \quad (20)$$

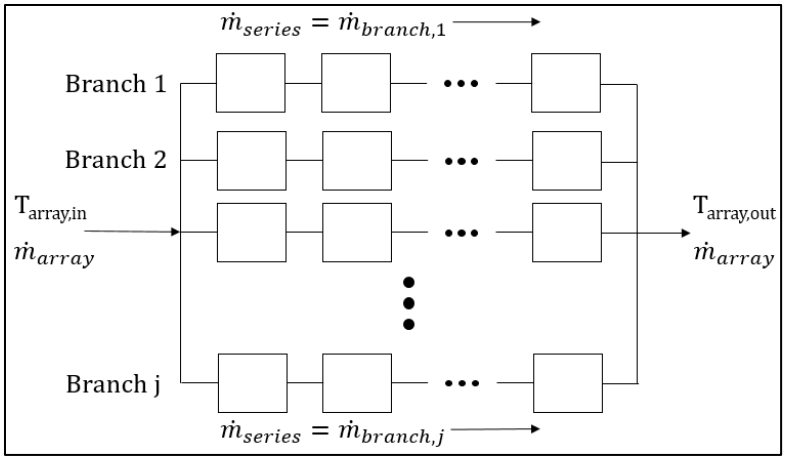

Figure 6: Schematic Diagram of Solar Collector Branches in Parallel

2.8 Thermal Energy Storage System

In hot summer months, cooling may be desired after the sun sets. Without the sun, the collectors have no irradiation to absorb, and stop contributing to the system. For this reason, thermal energy storage is required to heat the generator at night. Hot water storage tanks provide a means for storing thermal energy collected by the solar collector array during the day. These tanks are used as an intermediate point between the collector array and the generator. This allows the tank, or tanks, to gain heat from the collector array during the day, and provide the heat exchanger to the generator with hot water at a constant temperature. The energy balance for each tank is given by [15, 39]:

$$(mC_p)_s \frac{dT_s}{dt} = \dot{Q}_u - \dot{Q}_{load} - \dot{Q}_{loss} = \dot{Q}_u - \dot{Q}_{load} - (UA)_s(T_s - T_{a,tank}) \quad (21)$$

Where $\dot{Q}_u$, $\dot{Q}_{load}$, and $\dot{Q}_{loss}$ are the heat transfer rate into the tank by the collector array, the heat transferred out of the tank for the generator load, and the heat transferred to the surroundings through the shell of the tank respectively. $(UA)_s$ is the overall heat transfer

coefficient – area product for the tank, and m is the mass of water in the tank. T_s is the temperature of water in the tank, and $T_{a,tank}$ is the temperature of the around the tank.

In case of change of available solar irradiation due to cloudy or rainy weather, day-night cycles, and the passing of seasons; auxiliary heaters are in place to pick up the water heating demand if the collector array cannot provide necessary heating [38]. The auxiliary heat, $\dot{Q}_{aux}$,is added after the flow leaves the solar collectors. The temperature of the hot water tank can be observed over time by employing [39]:

$$T_s^+ = T_s + \frac{\Delta t}{(mC_p)_s}[\dot{Q}_u - \dot{Q}_{load} - (UA)_s(T_s - T_{a,tank})] \quad (22)$$

Where T_s^+ is the new tank temperature, and Δt is a period of time in seconds.

2.9 Heat Exchangers

Heat exchangers function to transfer heat from one fluid to another fluid without mixing the fluids. This is achieved by passing the fluid through pipes that share a common surface to allow for heat transfer, as seen in Figure 7.

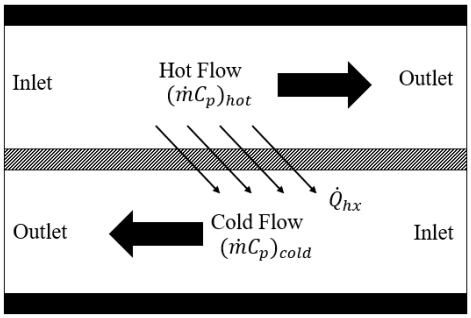

Figure 7: Fluid and Heat Flows through a Counterflow Heat Exchanger

There are many different types of heat exchangers. The counter-flow heat exchanger will be used for this analysis. A counter-flow heat exchanger has the hot and cold flows traveling in opposite directions. The heat transfer rate of the exchanger can be determined by the effectiveness-NTU method which is outlined below [41-43]:

$$\dot{Q}_{HX} = \varepsilon\left(\dot{m}C_p\right)_{min}(T_{hot\ in} - T_{cold\ in}) \quad (23)$$

Where the inlet capacitance rates $\left(\dot{m}C_p\right)_{hot}$ and $\left(\dot{m}C_p\right)_{cold}$ are compared; the lower product is assigned$\left(\dot{m}C_p\right)_{min}$, and the higher product is assigned $\left(\dot{m}C_p\right)_{max}$ respectively.

$$C^* = \frac{\left(\dot{m}C_p\right)_{min}}{\left(\dot{m}C_p\right)_{max}} \quad (24)$$

$$NTU = \frac{(UA)}{\left(\dot{m}C_p\right)_{min}} \quad (25)$$

Where UA is the overall heat transfer coefficient-area product, $C^*$is the capacitance rate ratio, NTU is the number of transfer units, and ε is the effectiveness of the heat exchanger [42].

$$\varepsilon = \frac{1-e^{-NTU(1-C^*)}}{1-C^*e^{-NTU(1-C^*)}} \quad \text{If} \quad C^* \neq 1 \quad (26)$$

$$\text{Or} \quad \varepsilon = \frac{NTU}{1+NTU} \quad \text{If} \quad C^* = 1 \quad (27)$$

The outlet temperatures of the hot and cold fluids can be found using the standard form of $\dot{Q}_{HX}$:

$$\dot{Q}_{HX} = \left(\dot{m}C_p\right)_{cold}(T_{cold\ out} - T_{cold\ in}) = \left(\dot{m}C_p\right)_{hot}(T_{hot\ in} - T_{hot\ out}) \quad (28)$$

CHAPTER 3: SUITABILITY, SIZING, AND CONFIGURATION OF A SOLAR POWERED VACS

This study covers the sizing of a 100RT LiBr-H_2O VACS as well as a thermal storage and transportation network located in Jackson, Mississippi USA; at approximately 32°N latitude [44].

3.1 Vapor Absorption Cooling System

The sample system has generator, condenser, evaporator, and absorber temperatures of 110, 50, 5, and 40 °C respectively; with high- and low-pressure components operating at 123.5 and 8.73 mbar respectively. The weak and strong solutions have LiBr concentrations of 0.578 and 0.66 by mass.

The system parameters defined above dictate the temperature, pressure, and concentration for all points in the VACS system excluding points 7 and 9, the outlets of the solution heat exchanger. The enthalpy for states 1 and 4 were calculated following the method shown in [45, 46], while the other states were calculated by the method presented in [29]. Table 1 summarizes the characteristics of the flow at each state point corresponding to Figure 3. The specific heat of the refrigerant for states 1 through 4 is unnecessary for calculation, and has not been included.

The information about the state points shown in Table 1 allows for the use of equations (2) through (12) to determine the mass flowrates through the vapor absorption system, shown in Table 2.

Table 1: Temperature, Pressure, Concentration, and Enthalpy of State Points for a 100 RT LiBr-H_2O VACS

State Point	Temperature, T (°C)	Pressure, P (mbar)	Mass Fraction LiBr, ξ (g LiBr/ g H_2O)	Enthalpy, h (kJ/kg)	Specific Heat, C_p (kJ/(kg*K))
1	110	123.5	0	2707	-
2	50	123.5	0	209	-
3	5	8.73	0	209	-
4	5	8.73	0	2509	-
5	40	8.73	0.578	106	1.95
6	40	123.5	0.578	106	1.95
7	87	123.5	0.578	199	2.01
8	110	123.5	0.66	283	1.80
9	52	123.5	0.66	182	1.73
10	40	8.73	0.66	161	1.70

Table 2: Evaporator Heat Rate and System Mass Flowrates for a 100 RT LiBr-H_2O VACS

Evaporator Heat Rate, $\dot{Q}_e$	100 RT (350kW)
Mass flowrate of Refrigerant, $\dot{m}$	0.1522 kg/s
Circulation Ratio, λ	7.05
Mass flowrate of Strong Solution, $\dot{m}_{SS}$	1.073 kg/s
Mass flowrate of Weak Solution, $\dot{m}_{WS}$	1.23 kg/s

With the mass flowrates of the VACS known, the effectiveness of the solution heat exchanger is found along with the outlet temperatures for states 7 and 9 by using the effectiveness-NTU method.

Table 3 presents the key values for the solution heat exchanger.

Table 3: Solution Heat Exchanger Hot and Cold Flow Characteristics and Effectiveness for a 100 RT LiBr-H_2O VACS

Crossflow Heat Exchanger Characteristics	Cold Flow	Hot Flow
Inlet Temperature, T_{in} (°C)	40	110
Mass Flowrate, $\dot{m}$ (kg/s)	1.22	1.07
Specific Heat, C_p (kJ/(kg*K))	1.95	1.80
Capacitance Rate, $\dot{m}C_p$ (kW/K)	2.39	1.93
Capacitance Rate Ratio, C^*	0.81	
Overall Heat Transfer Coefficient-Area Product, UA (kW/°C)	6.5	
Number of Transfer Units, NTU	3.37	
Effectiveness, ε	0.83	
Heat Transfer Rate of Exchanger, $\dot{Q}_{HX}$ (kW)	111.55	
Outlet Temperature, T_{out} (°C)	87	52

With the mass flowrates and enthalpies known at each state, the flow of heat into and out of each component is calculated, as presented in Table 4.

Table 4: Heat Rates for Main Components

Generator Heat Rate, $\dot{Q}_g$ (kW)	472
Condenser Heat Rate, $\dot{Q}_c$ (kW)	380
Absorber Heat Rate, $\dot{Q}_a$ (kW)	425

3.2 Generator – Hot Water Tank Heat Exchanger

The heat transfer rate and generator temperature are achieved and maintained by passing the LiBr-H_2O solution through a heat exchanger or a system of heat exchangers, Figure 8.

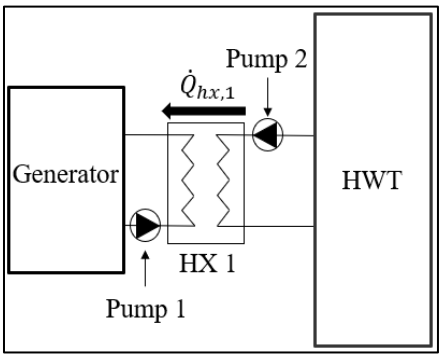

Figure 8: Schematic Diagram of Generator - Hot Water Tank Heat Exchanger System

The generator and the hot water tank act as the cold and hot sides of the heat exchanger respectively. The cold side inlet temperature for this demonstration is taken to be that of the weak solution entering the generator. The operating conditions of the selected fluid pumps, heat exchanger, and hot water tank determine the mass flowrate, temperature, and pressure ranges of the fluids, Table 5. The overall heat transfer coefficient-area product, UA, is dependent on the selected heat exchanger and fluid flows. The overall heat transfer coefficient depends on the material that the heat exchanger is made of, the geometry of the exchanger, and the flowrate and temperature of each fluid; while the surface area of the heat exchanger varies with design geometry. The various designs and operating conditions of heat exchangers, make the overall heat transfer coefficient-area product unique. Therefore, an assumption for the UA for the heat exchanger in this paper is assumed to be 6.5 kW/°C.

Table 5: Thermal Network Component Operating Characteristics

Characteristics	Fluid Pumps	Heat Exchangers	Hot Water Tank
Maximum Temperature, °C	343	232	200
Maximum Pressure, kPa	382	1034	1034
Maximum Mass Flowrate, kg/s	4.1	6.6	-
Overall Heat Transfer Coefficient-Area Product, W/°C	-	6500	11.1
Volume, m^3	-	-	0.3

3.2.1 Number of Generator – Hot Water Tank Heat Exchangers

For the heat transfer requirement of the generator to be met, there must be an adequate number of heat exchangers. In cases that the operating characteristics of a single pump and heat exchanger system cannot deliver the required heat, more must be added in parallel. The delivery of heat to the generator to achieve the desired temperature change between the heat exchanger inlet and outlet is dependent upon the mass flowrate through the cold side of the heat exchanger.

$$\dot{m}_{cold,req.} = \frac{Q_g}{C_{p,cold}(T_{cold,out} - T_{cold,in})} \quad (29)$$

The determination of the minimum number of heat exchangers is dependent upon the maximum achievable cold side flowrate through the heat exchanger; the lower of the maximum flowrates between the fluid pump and the heat exchanger.

$$Number\ of\ HX1 = \frac{\dot{m}_{cold,req.}}{\dot{m}_{cold,max}} \quad (30)$$

The mass flowrate through each of the heat exchangers is then an equal portion of the required mass flowrate, and the heat transfer requirements of each heat exchanger are reduced accordingly.

$$\dot{m}_{cold,hx1} = \frac{\dot{m}_{cold,req.}}{Number\ of\ HX1} \quad (31)$$

$$Q_{hx,1} = (\dot{m}_{cold,hx1} C_{p,cold})(T_{cold,out} - T_{cold,in}) \quad (32)$$

3.2.2 Hot Side Flow Operating Temperature and Mass Flowrates

With the heat transfer rate requirements and the cold side flow conditions of each heat exchanger known, the operating conditions of the hot side flow and the hot water tank can be investigated. Figure 9 illustrates the effect of the mass flowrate of the hot side flow on the hot flow inlet temperature requirements to deliver a prescribed heat transfer rate when the cold side flow remains constant, based on Equation 23. It can be seen that by increasing the mass flowrate of the hot side flow, the required inlet temperature is decreased; conversely, a slower flowrate requires higher temperatures to maintain the heat transfer rate. Examining the maximum flowrate of the hot flow side, the minimum temperature of the hot water tank can be determined. Similarly, if the temperature of the hot water tank increases above the minimum temperature, the mass flowrate of the hot side can be reduced to maintain constant heat transfer rate. With the knowledge of the maximum temperature of the hot water tank and other components, a minimum mass flowrate can be determined.

It can be seen that when the mass flowrate of the hot side is low, and the hot flow is C_{min} the effectiveness of the heat exchanger sharply falls with increasing mass flowrate, until the hot

flow becomes C_{max}, at which point the effectiveness slowly increases. This shows that if the heat exchanger and hot flow pump can withstand and provide a higher mass flowrate, the hot water tank can operate at lower temperatures, which would require less input heat to the tank. However, as the mass flowrate increases, the decrease in required temperature per increase in flowrate is reduced, allowing for a practical limitation of mass flowrate to be chosen.

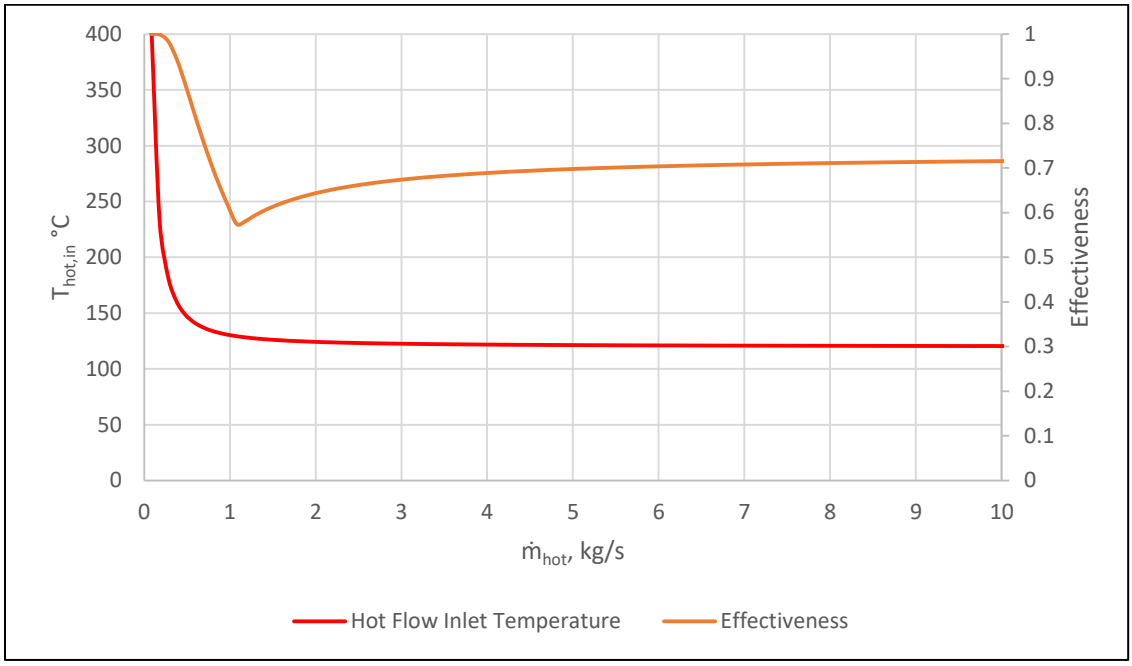

Figure 9: Effect of Altering Hot Flow Mass Flowrate on Hot Flow Inlet Temperature and Heat Exchanger Effectiveness

Calculation of hot water tank temperature for a given mass flowrate requires the use of the specific heat of the water in the tank, which is a function of temperature. Therefore, a method of approximation is required to determine both the temperature of the hot water and its specific heat. The Newton method was employed for this work. The results of this method for the minimum and maximum temperatures are shown in Table 6.

Table 6: Maximum and Minimum Flowrate Characteristics for Generator – Hot Water Tank Heat Exchanger Hot Side Flow

Flowrate Characteristics	Maximum Mass Flowrate	Minimum Mass Flowrate
Mass Flowrate	3	0.2336
Temperature, °C	122	200
Specific Heat, J/(kg*°C)	4247.2	4497.1

3.3 Sizing of Solar Collector Array

Based on the location of the system, the solar irradiation available at a given time of year and day changes, as does the temperature. Due to this the performing a study of the expected conditions is an important step when assessing the size and practicality of a solar collector field. A study of the hourly solar irradiation over an average day of the month for the local latitude was performed [29], and the local yearly temperatures from 1981 to 2010 were gathered [47]. Figure 10 shows the compilation of solar irradiation over a year, and Figure 11 shows the expected temperature range over a year. Figure 10 shows the solar irradiance with respect to the solar hour of the day. Solar time is based around solar noon, which is when the sun is directly overhead. Each solar hour after that is determined by the sun moving approximately 15.2° from the local meridian line [31, 34, 48]. Once the sun is below the horizon as seen from the location, the solar irradiance is reduced to zero until the sun rises the next day. This analysis uses the average high temperature of the month due to the useful working hours of the solar collector array coinciding with the times of solar irradiance, and thereby the hotter hours of the day.

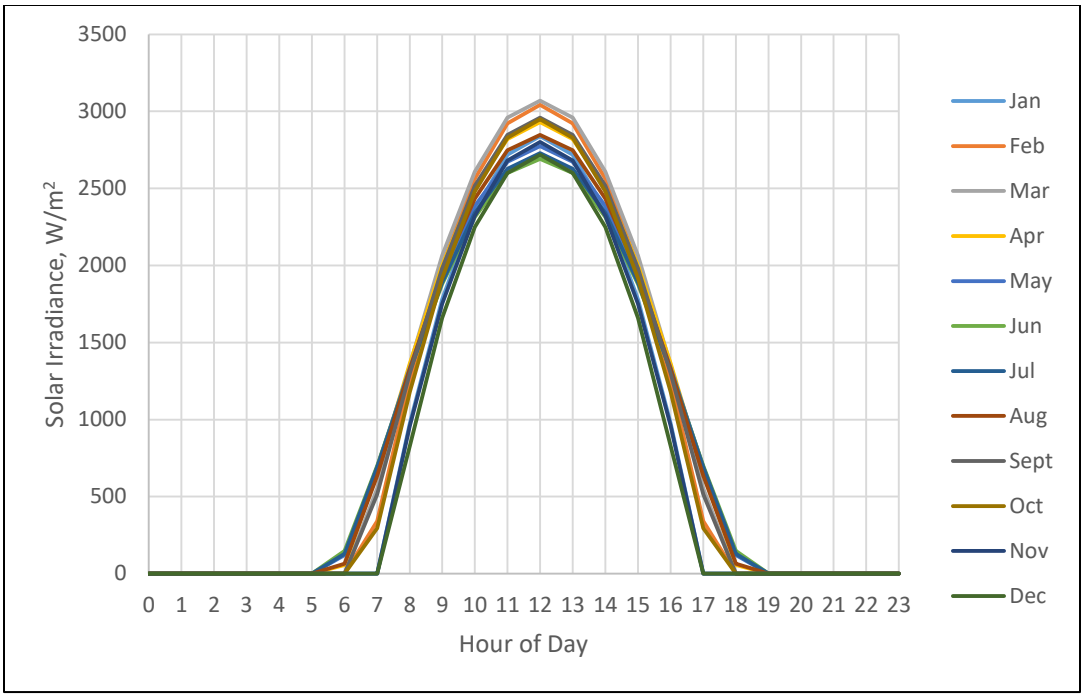

Figure 10: Hourly Solar Irradiation by Representative Day of the Month for Jackson, MS

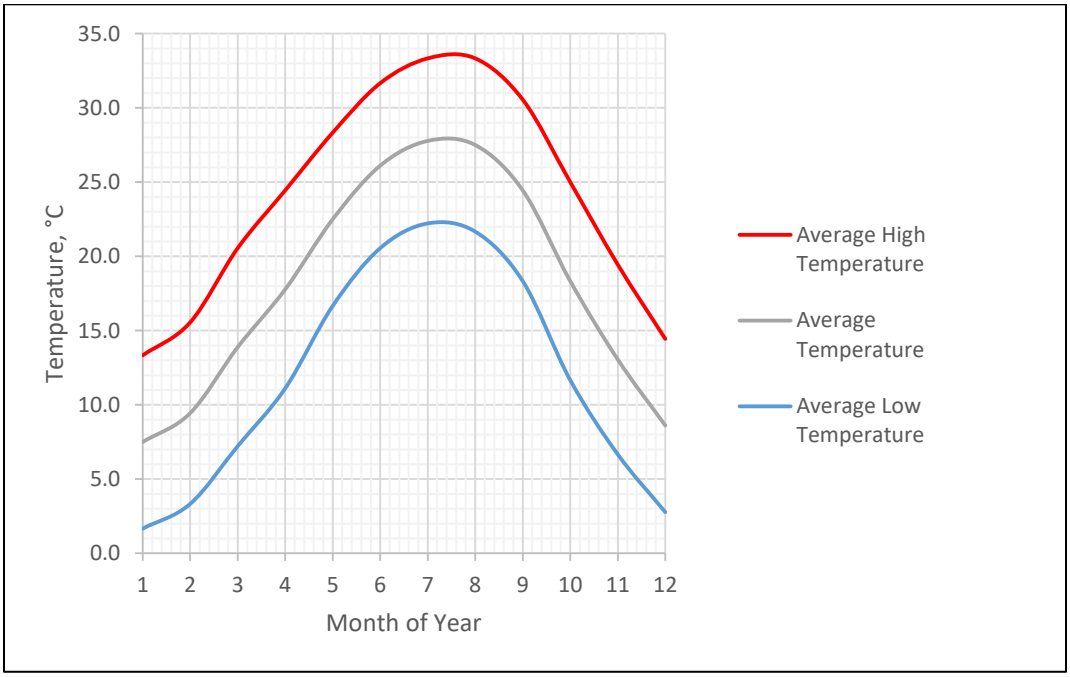

Figure 11: Average Temperature by Month of Year for Jackson, MS

A flat-plate collector was chosen for this analysis due to the popularity, ease of use, and lower cost per unit than compound parabolic concentrating collectors or vacuum tube collectors. The method of analysis would be the same for those collectors, and would likely required fewer collectors overall due to their concentrating nature allowing them to attain higher temperatures from less irradiation, and being able to withstand a higher temperature range overall. The data for the collectors used in this analysis is shown in Table 7.

Table 7: Characteristics of Flat Plate Solar Collector Model

Heat Transfer Fluid	50% Propylene-Glycol
Max. Operating Temperature, T_{max}(°C)	276
Max. Pressure, P_{max} (kPa)	275
Transmissivity, τ	0.92
Absorptivity, α	0.95
Heat Removal Factor, F_R	0.855
Overall Conductance, U_L (W/°C m^2)	3.322
Mass Flowrate, $\dot{m}_{series}$ (kg/s)	2.21E-02

Solar collectors in series enable the solar collector array to reach higher temperatures because the outlet of one collector is the inlet to the next. As the number of collectors increases, the temperature of the propylene-glycol increases, which reduces the ability of the next collector to impart heat, Figure 12. This trend continues until the amount of heat absorbed by the collector is equal to the increased heat lost by the collector, resulting in maximum temperature gain that can only be increased by increasing the solar irradiation or decreasing the mass flowrate through the collectors. This is attributed to the increase in the product of the conductive heat loss

coefficient and the temperature difference from the fluid temperature and the ambient temperature, $U_L(T_{in} - T_a)$, as shown in Equations 16, 17, and 18.

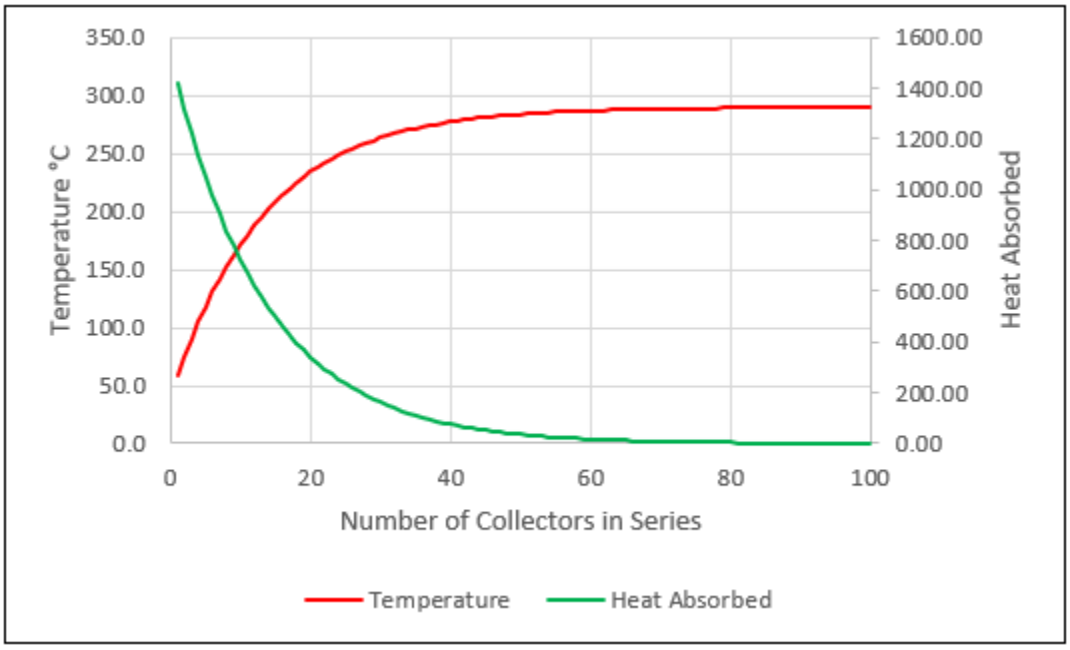

Figure 12: Temperature and Heat Absorption Limitations with Series Solar Collectors

When determining the maximum outlet temperature of the solar collector array, it is important to take the maximum temperatures and pressures of the fluid pumps and the heat exchangers, as well as the changing solar irradiation and ambient temperature throughout the year. The operating conditions of the solar collector are determined by the collector's maximum operating pressure. This is because the collectors are designed to be connected and used in a system. To determine the maximum operating temperature of the solar collector, the pressure must be related to the temperature through equations of state. The pressure to temperature relationship for propylene-glycol is [49]:

$$T_{max,sca} = \frac{2692.187}{6.07936 - \log(P_{max,sc})} + 17.94 \quad (33)$$

Taking the operating temperature and pressure of the components working with the propylene-glycol into account, the maximum allowable temperature of the solar collector array – hot water tank heat exchanger can be determined.

To ascertain the number of solar collectors in series for a given maximum allowable temperature, operation of the system under all solar irradiance and temperature conditions is required for the year is required. Figure 13 shows the temperature range of 23 collectors in series throughout a day in March with a collector inlet temperature of 20°C, where maximum temperature out of the array can be seen to be 231 °C at solar noon, which can be determined using Equations 16, 17, and 18. This analysis is required for each month to ensure that the change in ambient temperature does not overcome the lack of solar irradiation in any case.

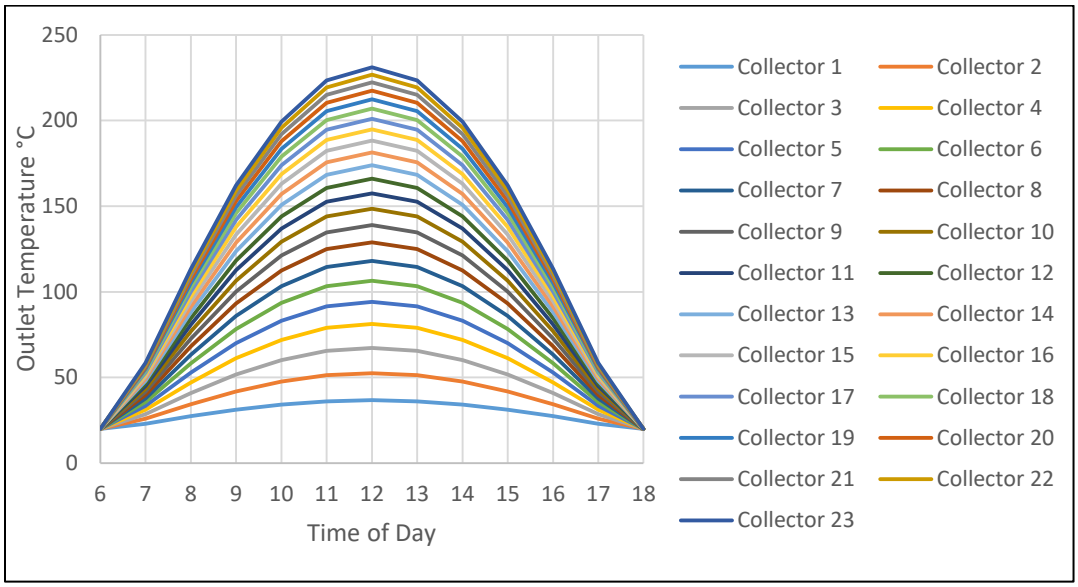

Figure 13: Outlet Temperatures of Series Collectors Over a Day in March for Jackson, MS

The appropriate number of solar collector branches is determined by the required heat transfer rate through the heat exchanger. Before solar collector array can be configured, the number of solar collector array – hot water tank heat exchangers must be discerned, which is

dependent upon the demand of heat compared to the availability of heat from the solar collector array. The minimum amount of heat required from the solar collector array would occur when the hot water tank is at minimum temperature. This provides the scenario for least heat loss to the surroundings for the hot water tank, paired with addition to the heat being transferred out of the hot water tank to the generator through the generator – hot water tank heat exchanger, and can be calculated as shown below.

$$\dot{Q}_{hx,2} = \dot{Q}_{hx,1} + \dot{Q}_{Loss} \quad (34)$$

The ability of a heat exchanger to meet this demand is dependent upon the temperature of the hot side flow from the solar collector array and the mass flowrates of each side of the heat exchanger. As shown in Figure 9 and Equation 28, to achieve the highest amount of heat transfer from the solar collector array through the heat exchanger, the condition for the maximum number of solar collector branches and thereby, maximum hot side flowrate, must be defined. For this, the maximum mass flowrates of the solar collectors and the heat exchanger are considered, so that the sum of the flowrates through each branch approaches the maximum flowrate capacity of the heat exchanger.

$$Maximum\ Number\ of\ Branches\ per\ Heat\ Exchanger = \frac{\dot{m}_{max,hx}}{\dot{m}_{max,sc}} \quad (35)$$

The effects of altering the mass flowrate of the cold side flow while maintaining constant heat transfer and cold flow inlet temperature is examined in Figure 14 and Equations 23 and 28. It can be seen that as the mass flowrate of the cold side flow is reduced, the temperature of the cold outlet flow increases with the temperature demand of the hot inlet flow. As the effectiveness of the heat exchanger tends toward unity, the outlet temperature of the cold flow approaches that of the hot flow inlet temperature. To determine the maximum amount of heat transfer for this

case, the lowest temperature input from the hot side flow should be considered, which coincides with the use of the maximum mass flowrate for the cold side flow.

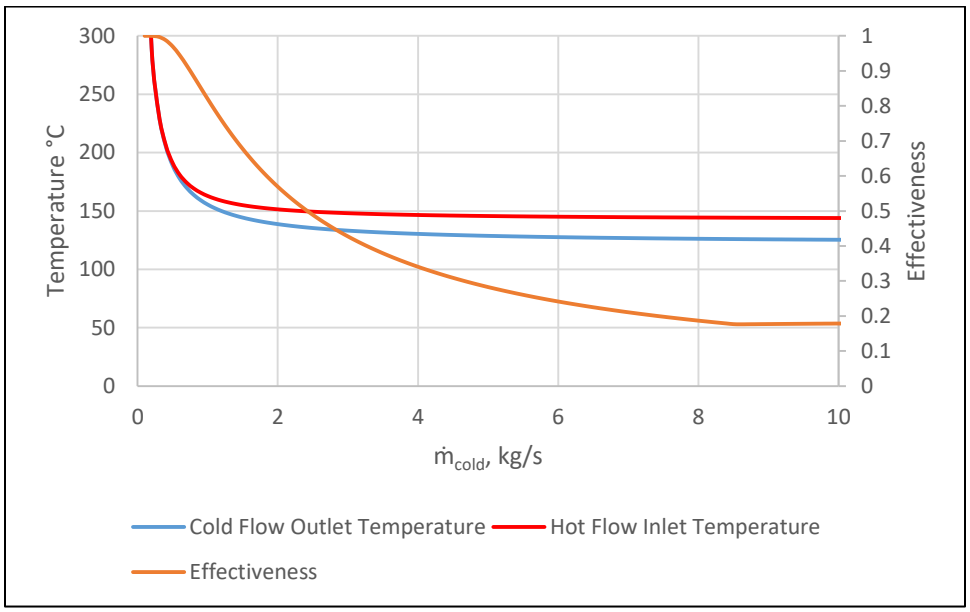

Figure 14: Effect of Cold Flow Mass Flowrate on Cold Flow Outlet and Hot Flow Inlet Temperatures and Heat Exchanger Effectiveness

Using the maximum mass flowrate conditions for both hot and cold flows and using the maximum number of collectors in series, the maximum heat transfer rate of the heat exchanger is determined. If the maximum heat transfer rate of the heat exchanger does not meet the requirements of the hot water tank, then additional heat exchangers in parallel are needed, Figure 15; with each additional heat exchanger splitting the heat transfer requirements of the system proportionally.

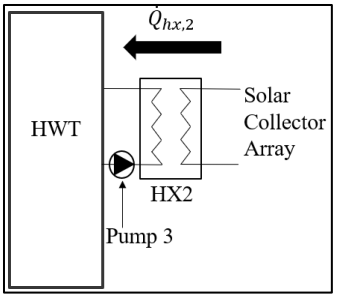

Figure 15: Schematic Diagram of the Hot Water Tank - Solar Collector Array Heat Exchanger System

Knowing the heat transfer requirements of the hot water tank, and the operating temperature ranges and flowrate ranges of the hot water tank and the fluid pump, the sizing of the solar collector array can begin. For the maximum amount of heat input from the solar collector array, the largest solar collector array is required. However, using the largest possible solar collector array may not be reasonable due to the space requirements or allotted expenditures for the proposed system. The optimization of the solar collector array for size and heat deliver becomes unique and dependent upon the desired operating conditions and space availability of the system. Collector in series allow for higher temperatures, while collectors in parallel create a higher mass flowrate through the heat exchanger; each case having an opportune usage. Systems that require high temperatures from the collector array, will intrinsically require a high number of collectors in series. To increase the heat transfer, branches would be added; and for each branch, the number of collectors in series is added to the total number of collectors used. This quickly increases the cost and space requirements for the system. Alternatively, an investigation of using additional collectors in series can be performed; to where adding 5 collectors in series to a line of 20 collectors requires less than adding another branch of 20 collectors. For systems that require lower temperature ranges, that can be met with only a few collectors in series, the addition of branches may result in lower overall requirement of collectors. For instance, if the temperature requirement can be met by 3 collectors in series, but

either an additional branch or 5 additional collectors in series are required to necessitate the heat transfer rate, the additional branch requires fewer overall collectors. The configuration of the solar collector array also impacts the systems required auxiliary heating demand, as arrays with higher numbers of collectors in series will achieve higher temperatures of the hot water tank sooner in the day, as evidenced by Figure 13.

This case limits the size of the solar collector array to no more than 1000 collectors due to space and investment constraints. For this system to achieve maximum heat transfer, since the temperature of the hot water tank is high, the number of collectors in series are maximized, and branches are added evenly to each solar collector array – hot water tank heat exchanger. This arrangement results in 10 branches of 23 solar collectors in series for each hot water tank, culminating in a total of 920 collectors. This limitation of the number of collectors reduces the amount of heating that the solar collectors can provide to the system. Figure 16 compares the heat sources of the solar collector array to the auxiliary heater for the month of March, using a representative day of the month which accounts for average solar irradiance. The sum of the heat sources shown equates to the heat transfer requirement of the generator – hot water tank heat exchanger as well as the heat transferred to the surroundings. Due to the influx of solar irradiance not surpassing the minimum heat requirement for heating the water above the minimum temperature, the temperature of the tank remains constant; being maintained by the auxiliary heater at 122 °C.

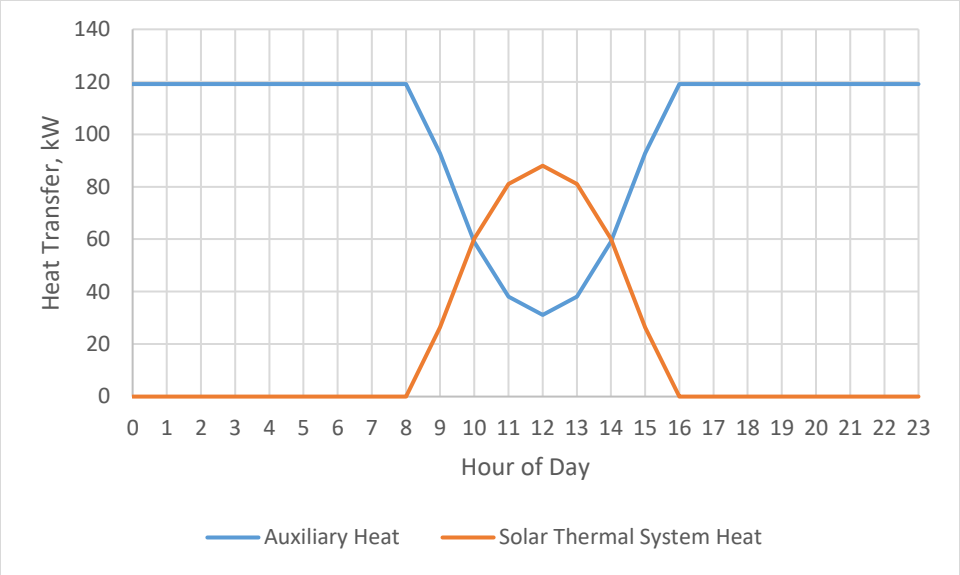

Figure 16: Comparison of Heat Inputs to the Hot Water Tank for the Month of March

A similar analysis was performed over the span of a year, Figure 17, using representative a representative day of each month. The heat input from each source per representative day is shown are included in Table 8.

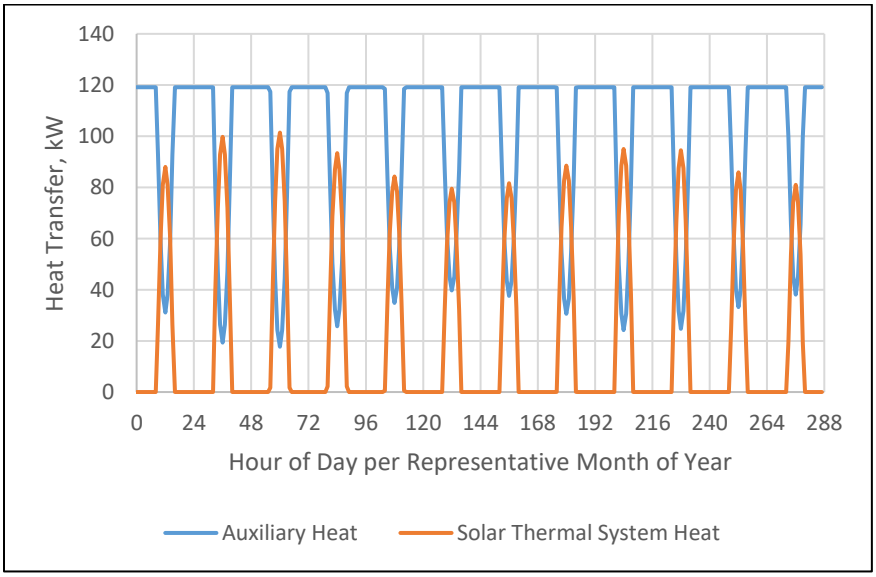

Figure 17: Comparison of Heat Input to Hot Water Tank Over a period of One Year

It can be seen in Table 8 that the solar collector array produced between 15-20% of the heat input to the hot water tank per month. Although constraining the number of solar collectors reduced the potential heat input to the system during daylight hours, the majority of the auxiliary was consumed during non-daylight hours. For this reason, VACS are typically paired with a VCCS to be run at night. The typically low coefficient of performance of VACS is a non-issue during daylight hours when paired with solar collectors due to the thermal energy provided by the sun being responsible for a large portion of the heating requirements. However, during night hours and for VACS requires a large amount of thermal energy provided solely by the auxiliary heater. Smaller capacity VACS may be able to take advantage of the hot water tanks to allow for additional energy savings into the night, but due to the high demand of heat by the generator and the small volume of the hot water tanks used in this case, the heat capacitance of the hot water tank negligible.

Table 8: Daily Total of Heat Input to Hot Water Tank Over a period of One Year

Month (hours)	Auxiliary Heat (kW day)	Solar Heat Transferred to Tank (kW day)
Jan (0-23)	2436	423
Feb (24-47)	2351	508
Mar (48-71)	2329	530
Apr (72-95)	3044	530
May (96-119)	2424	436
Jun (120-143)	2452	407
Jul (144-167)	2442	417
Aug (168-191)	2403	456
Sep (192-215)	2372	487
Oct (216-239)	2387	472
Nov (240-263)	2450	409
Dec (264-287)	2484	375
Yearly Total (MWh)	3598	662

CHAPTER 4: LIFE CYCLE ASSESSMENT OF HEAT SOURCES FOR VACS

A Life Cycle Assessment (LCA) is a technique for analyzing the environmental impacts associated with a product or service throughout its life [50]. This process has been standardized by the family of ISO 14040 standards. The application of this technique requires Goal and Scope Definition (GSD), Life Cycle Inventory analysis (LCI), Life Cycle Impact Assessment (LCIA), and Interpretation of assessment results [50-52]. The GSD of a study defines the intended application and audience, functional unit, impact categories of interest, type of LCA, system boundaries, and assumptions and limitations of the assessment. The LCI gathers data for resources and energy used and emissions and products created from each process, and establishes a model to simulate the system and calculate the mass and energy flows within and between system boundaries [52]. The LCIA predicts the potential environmental impacts of a product or process by investigating the materials, energy, transportation, and production methods described in the LCI [52].

4.1 Goal and Scope Definition

The goal of this study is to investigate methods of supplying thermal energy to the VACS described in Chapter 22. By determining which methodology of delivering heat to the VACS requires the least amount of energy and material while producing the least amount of pollution and waste, the environmental impacts of using VACS will be reduced as industries supplying the

superior method with be bolstered. This study will analyze the use of a solar thermal network, wood pellet power, and coal power to deliver a required heat rate to the cooling system.

Goals of this analysis:

- Determine material and energy costs for given heat source
- Analyze the environmental impact associated with these systems from cradle-to-grave
- Evaluate if there is a trade-off between the environmental effects of these systems

A comparative cradle-to-grave approach was conducted in this assessment, utilizing data encompassing the full life cycle of each component process. The ecoinvent database version 3.2 was employed in this analysis utilizing openLCA software version 1.7. The Tool for the Reduction and Assessment of Chemical and other environmental Impacts (TRACI) assessment method is utilized to assess the impacts resulting from the production of each component process. TRACI was developed for process in the United States, which applies input parameters U.S. locations for the span of 100 years [53].

4.1.1 Functional Unit

The functional unit is used to define the system under study, and serves to present the results in an easily comparable form [54]. The selection of the functional unit is challenging for this case, due to the solar collector not having a pre-determined energy density. However, system sizing has been provided for this system and thereby the number of collectors and hot water tanks is known. Comparing the amount of heat absorbed over a year allows for the determination

of required annual auxiliary power. Therefore, the functional unit will be the amount of energy (MJ) required to operate to system, including disposal of all heat sources.

4.1.2 Impact Categories

A common impact between all presented forms of heat generation is the contribution to global warming at some stage of life cycle. Therefore, the primary impact category under investigation is the global warming potential measure in units of equivalent kg of CO_2.

4.1.3 Type of LCA

This study is aimed to investigate the environmental impacts caused by use of various heat and energy sources. Due to the change in heat sources, this is a consequential LCA. A consequential LCA investigates the impacts associated with altering a product or process; therefore, the inclusion of components that remain constant between cases is not necessary.

4.1.4 System Boundary and Cut-off Criteria

The characteristic contrast between the heating sources requires unique system boundary definition per case.

Solar Thermal System – The large number of constituent components required for the material extraction, manufacturing, and assembly of each component and the system as a whole have roots too far reaching for a practical consequential analysis of this level. For that reason, the

key components included in the analysis of the solar thermal system are the solar collectors and hot water tanks. Where the assessed life cycle consists of three stages: construction, operation, and decomposition.

Wood Pellet Power – The production of wood pellets consists of silviculture and logging operations, wood pellet production, transportation and the combustion of these pellets at a wood pellet power plant completes the life cycle.

Coal Power – The production of coal power includes mining, refining, transportation, and combustion.

The energy and resources required for the construction of facilities to and capital equipment for each of these systems is beyond the scope of this report. It is assumed that the environmental impacts of production and combustion facilities are small in comparison to the number of units produced during the lifetime of these facilities.

4.2 Life Cycle Inventory Analysis

The solar thermal system is composed of solar collectors and hot water tanks in an arrangement to deliver heat over the course of the day, depending on solar irradiation. The flat-plate collector and hot water storage tanks assessed by Ozturk et al. (2012) were assumed comparable to those described in the system, with the hot water tank having a similar mass to that described by Comodi et al. (2016) the volume of the tank is estimated to be approximately 300 liters. The weight, energy usage, and CO_2 production associated with the system; assuming

recycling, maintenance, transportation, and other are closely connected with the number of solar collectors.

Table 9: Mass, Manufacturing Energy, and CO2 Emissions for Solar Thermal System

System Component / Operation	Mass of Component (kg)	Primary Use Energy (MJ)	CO_2 Emission (kg)
Solar Collectors	56948	3406760	184000
Hot Water Tanks	318.8	17804	196
Support Structures	25300	1006480	15640
Metal Recycling	-	708400	23920
Maintenance	-	1219920	41400
Transportation	-	318320	13800
Other	-	358800	34960
Total	82566.8	4431044	199836

By observing the use of the system over the span of a year, the amount of useful heat and required auxiliary heat can be found to be approximately 3.6 GWh per year. The auxiliary heating of the system is assumed to be delivered by an electric heater with no heat loss due to efficiency. The auxiliary heater can be powered by wood pellet or coal power. The heat of combustion for wood pellets and coal is shown in Table 10 [53, 55]. The efficiency of the power plant is assumed to be approximately 34% [53, 55]. Consumption of wood pellets and coal required per year and over the lifetime of the system for solar thermal auxiliary heat and as the primary heating source are shown in Table 11. The starting location, distance traveled to Jackson, and the method of transportation for each component is summarized in Table 12.

Table 10: Heat of Combustion of Wood Pellets and Coal

Power Source	Heat of Combustion (MJ/kg)
Wood Pellet	17.3
Coal	25.12

Table 11: Power Source Consumption

Heat Source	Annual Consumption Auxiliary Heating (metric ton)	Annual Consumption Primary Heating (metric ton)
Wood Pellets	2202	2531
Coal	1517	1743

Table 12: Transportation Information

Transportation Information	Solar Collector	Hot Water Tank	Wood Pellets	Coal
Starting Destination	Bainbridge, NY	Bainbridge, NY	Lucedale, MS	Illinois
Distance to Jackson, MS	2000 km	2000 km	238 km	1538 km
Method of Transportation	Semi-truck	Semi-truck	Semi-Truck	Railroad

4.3 Life Cycle Impact Assessment

Using openLCA the life cycle impact assessment of the transportation for each case is considered on a unit basis for one-way delivery, Table 13.

Table 13: Global Warming Potential for per Unit of System and Power Source for Jackson, MS

Element and Amount of Heat Source	kg of CO_2 Due to Transportation
Single Solar Collector	21.7
Single Hot Water Tank	28
Metric Ton of Wood Pellets	64.2
Metric Ton of Coal	41.78

Using a conservative estimate for the life of the solar thermal system (STS) as 10 years, the global warming potential of one life time of the STS can be examined with both sources of auxiliary heat, Table 14.

Table 14: Global Warming Potential of Solar Thermal System over 10-year Life

Element and Amount of Heat Source	Metric Tons of CO_2
Solar Thermal System	220
Auxiliary Wood Pellet Power	4644
Auxiliary Coal Power	42371
Primary Wood Pellet Power	5345
Primary Coal Power	48683

The information presented in Table 14 represents 10 years of time, after which the system will be replaced by an identical system. Table 15 showcases the 100-year TRACI analysis.

Table 15: Global Warming Potential Due to Heat and Power Sources over 100 Years

Environmental Impact	Auxiliary Wood Pellet Power	Auxiliary Coal Power	Wood Pellet Power	Coal Power
Global Warming Potential (metric tons of CO_2)	48636	425905	53449	486826

It is apparent from the results that the use of the solar thermal system in combination with the wood pellet power plant allows for the least global warming potential, followed by the solar and coal combination. This is, in part, due the location of the wood pelletizing plant being close to the wood pellet power plant; however, the primary reason for the difference is the amount of CO_2 produced during the burning of each fuel. For every kWh of electricity, coal produces 1.16 kg CO_2-eq. compared to 0.09 kg CO_2-eq. for wood pellets [53].

4.3.1 Energy Payback Time

Energy payback time (PBT_E) of renewable energy sources allows for evaluation of ecological and environmental performance [56], and is given below.

$$PBT_E = \frac{LCA_{energy}}{E_{useful} - E_{use}} \qquad (36)$$

Where LCA_{energy} is the primary energy consumed during all life cycle phases, E_{useful} is the yearly useful saved energy, and E_{use} is the energy consumed during the use of the system. The energy savings of the system is referring to the use of the solar collector array, which by saving 662 MWh over the course of a year has an energy payback period of approximately 1.9 years.

4.3.2 CO_2 Payback Period

The global impacts of the system, life cycle and emissions saving are summarized by the CO_2 payback time [56].

$$PBT_{CO_2} = \frac{CO_{2,eq-i}}{(CO_{2,eq-S}) - (CO_{2,eq-use})} \qquad (37)$$

Where $CO_{2,eq\text{-}I}$ is the global emissions in terms of tones of CO_2-equivalent pollution related to the manufacturing, upkeep, and recycling of the solar thermal system, $CO_{2,eq\text{-}S}$ is the amount of CO_2 equivalent pollution avoided by using the system, and $CO_{2,eq\text{-}use}$ is the equivalent pollution required to operate the system. To allow for this calculation, a comparison to an alternative system must be made. When compared to a domestic gas boiler used as an auxiliary system with an assumed specific global warming factor of 65.7 kg CO_2-eq/GJ of heat produced, the payback period can be seen to be approximately 0.2 years.

CHAPTER 5: CONCLUSION AND FUTURE WORK

Vapor absorption cooling systems (VACS) offer a means of cooling which requires mainly low-grade thermal energy. A solar thermal system can be employed to meet the demand for thermal energy. The size and configuration of the solar thermal system is dependent upon the operating conditions of the components which comprise the system, as well as the cooling demand of the system. A practical approach of determining the size and configuration of a solar thermal system to meet the cooling demand of a VACS was investigated. For the sample 100 RT VACS located in Jackson, MS, USA with the selected components and system size limited to 1000 collectors the system requires these components: 4 heat exchangers in parallel with the VACS generator, 4 hot water tanks, 1 heat exchanger per hot water tank, and 920 solar collectors with 23 collectors in series and 10 branches per solar collector array – hot water tank heat exchanger.

A consequential life cycle assessment was carried out for the described system to compare the environmental impacts of the solar thermal system to that of using a heating coil in the generator of the VACS powered by wood pellet or coal power. Through this analysis it was evident that the use of the solar thermal system required less energy and produced less CO_2 than either wood pellet power or coal power alone. The use of the solar thermal system subsidized by wood pellet power produces 10 times less CO_2 than that of the strictly coal powered system. The energy and CO_2 payback periods of the proposed solar thermal system were seen to be approximately 1.9 and 0.2 years respectively.

The goal of this work was to investigate a new method of approach in the sizing of solar powered VACS, designing a solar thermal system to meet the heating demand of the VACS, as opposed to designing the VACS around the solar thermal system. Being new, this method is not perfect; requiring assumptions and needing further optimization. The assumptions of specific heat for the cold side flows can be improved by the addition of an iterative calculation to converge on an appropriate approximation for both water and propylene glycol based on operating temperatures. Additionally, the heat transfer through the system can be optimized by altering the flowrates through the heat exchanger throughout the day; allowing for improved heat transfer to and heat retention of the hot water tank. The investigation into photovoltaic cells can be investigated as an energy source to meet the auxiliary heating demand. Modeling of this system in TRANSYS or a similar transient modeling software would allow for more accurate and real time data analysis, as would constructing a small-scale model.

LIST OF REFERENCES

[1] L. Chen, Y.-M. Chen, M.-H. Sun, Y.-L. Zhang and X.-R. Zhang, "Concept design and formation of a lithium bromidepwater cooling system powered by supercritical CO2 solar collector," *Energy Conversion and Management,* no. 85, pp. 313-322, 2014.

[2] O. W. Mohammed and G. Yanling, "Comprehensive Parametric Study of a Solar Absorption Refrigeration System to Lower Its Cut In/Off Temperature," *Energies,* vol. 10, no. 1746, 2017.

[3] U. Eicker, "Solar Cooling," in *Energy Efficient Buildings with Solar and Geothermal Resources,* United Kingdom, John Wiley & Sons, 2014, pp. 299-318.

[4] C. Borgnakke and R. E. Sonntag, in *Funamentals of Thermodynamics*, Hoboken, NJ, John Wiley & Sons, 2013, pp. 244, 433-443.

[5] J. Prisco, "Why it's time to redesign the old air conditioner," CNN, 2 December 2019. [Online]. Available: https://edition.cnn.com/style/article/global-cooling-prize-india/index.html. [Accessed 4 December 2019].

[6] B. Dean, J. Dulac, T. Morgan and U. Remme, "The Future of Cooling: Opportunities for energy-efficient air conditioning," OECD/IEA, 2018.

[7] M. Li, C. Xu, R. H. E. Hassanien, Y. Xu and B. Zhuang, "Experimental investigation on the performance of a solar powered lithium bromide-water absorption cooling system," *International Journal of Refrigeration,* no. 71, pp. 46-59, 2016.

[8] Global Cooling Prize, "World's leading AC manufacturers and innovative technology companies in running for the Global Cooling Prize," Global Cooling Prize, 2019. [Online]. Available: https://globalcoolingprize.org/finalist-global-press-release/. [Accessed 4 December 2019].

[9] U.S. Energy Information Administration, "What's New in How We Use Energy at Home," EIA, 31 May 2018. [Online]. Available: https://www.eia.gov/consumption/residential/reports/2015/overview/index.php. [Accessed 15 May 2019].

[10] U.S. Energy Information Administration, "Air Conditioning in nearly 100 million U.S. homes," EIA, 19 August 2011. [Online]. Available: https://www.eia.gov/consumption/residential/reports/2009/air-conditioning.php. [Accessed 30 May 2019].

[11] Energy Saver, "Air Conditioning," U.S. Department of Energy, [Online]. Available: https://www.energy.gov/energysaver/home-cooling-systems/air-conditioning. [Accessed 30 May 2019].

[12] E. I. Kharagpur, "Lesson 14: Vapour Absorption Refrigerant Systems," 2008. [Online]. Available: http://moreameya.weebly.com/uploads/1/7/7/6/17762229/refrigeration_and_air_conditioning.pdf. [Accessed 4 March 2019].

[13] H. A. Patel, L. Patel, D. Jani and A. Christian, "Energetic analysis of single stage lithium bromide water absorption refrigeration system," *Procedia Technology,* no. 23, pp. 488-495, 2016.

[14] S. M. Osta-Omar and C. Micallef, "Mathematical Model of a Lithium-Bromide/Water Absorption Refrigeration System Equipped with an Adiabatic Absorber," *Computation,* vol. 4, no. 44, 2016.

[15] E. D. Kerme, A. Chafidz, O. P. Agboola, J. Orfi, A. H. Fakeeha and A. S. Al-Fatesh, "Energetic and exergetic analysis of solar-powered lithium bromide-water absorption cooling system," *Journal of Cleaner Production,* no. 151, pp. 60-73, 2017.

[16] M. Chahartaghi, H. Golmohammadi and A. F. Shojaei, "Performance analysis and optimization of new double effect lithium bromide-water absorption chiller with series and parallel flows," *Inernational Journal of Refrigeration,* no. 97, pp. 73-87, 2019.

[17] Z. Li, L. Liu and J. Liu, "Variation and design criterion of heat load ratio of generatior for air cooled lithium bromide-water double effect absorption chiller," *Applied Thermal Engineering,* no. 96, pp. 481-489, 2016.

[18] S. Anand, A. Gupta and S. K. Tyagi, "Exergy Analysis of a LiBr-H2O Vapor Absorption Refrigeration Plant: A Case Study," *International Journal of Air-Conditioning and Refrigeration,* vol. 22, no. 2, 2014.

[19] I. Beausoleil-Morrison, G. Johnson and B. P. Kemery, "The experimental characterization of a lithium bromide-water absorption chiller and the development of a calibrated model," *Solar Energy,* no. 122, pp. 368-381, 2015.

[20] S. Bolocan, A. S. Florea Chiriac, G. Dragomir and G. Nastase, "Development of a small capacity solar cooling absorption plant," *Energy Procedia,* no. 74, pp. 624-632, 2015.

[21] E. I. Kharagpur, "Lesson 15: Vapour Refrigeration Systems Based On Water-Lithium Bromide Pair," 2008. [Online]. Available: http://moreameya.weebly.com/uploads/1/7/7/6/17762229/refrigeration_and_air_conditioning.pdf. [Accessed 4 March 2019].

[22] A. Behfar, Z. Shen, J. Lau and Y. Yu, "Heat and mass transfer enhancement potential on falling film absorbers for water-LiBr mixtures via a literature review (RP-14620," *HVAC&R*, no. 20, pp. 570-580, 2014.

[23] P. Coroyannakis, T. Tsoutsos and Z. Gkouskos, "Solar Cooling: Overview and Recommendations," SOLCO.

[24] M. Krolikoska and M. Zawadzki, "The experimental study on influence of zwitterionic compunds on solubility of lithium bromide in water," *Fluid Phase Equilibia*, no. 475, pp. 18-24, 2018.

[25] L. Weng, W. Song, D. J. Jacobs and G. D. Elliott, "Molecular insights into water vapor absorption by aqueou lithium bromide and lithium bromide/sodium formate solutions," *Applied Thermal Engineering*, no. 102, pp. 125-133, 2016.

[26] A. D. Lucas, M. Donate and J. F. Rodriguez, "Applying surfactants to improve the absorption capacity of mixtures of lithium bromide and formates in absorption refrigeration coolers," *International Journal of Refrigeration*, no. 31, pp. 1073-1080, 2008.

[27] "Ammonia - Thermophysical Properties," The Engineering Toolbox, 2008. [Online]. Available: https://www.engineeringtoolbox.com/ammonia-d_1413.html. [Accessed 4 December 2018].

[28] S. M. Osta-Omar and C. Micallef, "Effect of Vapour-Solution Interface Area on a Miniature Lithium-Bromide/Water Absorption Refrigeration System Equipped with an Adiabatic Absorber," *Energy Procedia*, no. 118, pp. 243-247, 2017.

[29] J. Patek and J. Klomfar, "A Computationally Effective Formulation of the thermodynamic properties of LiBr-H2O Solutions from 273 to 500 K Over Full Composition Range," *International Journal of Refrigeration*, no. 29, pp. 566-578, 2006.

[30] H.-M. Hellmann, "Improved Property Data Correlations of Absorption Fluids for Computer Simulation of Heat Pump Cycles," *ASHRAE Transactions*, pp. 980-997, 1996.

[31] B. K. Hodge, "Active Solar Thermal Applications," in *Alternative Energy Systems and Applications*, USA, John Wiley & Sons, Inc., 2010, pp. 149-190.

[32] G. Ampuno, L. Roca, M. Bergenguel, J. D. Gil and P. Manuel, "Modeling and simulation of a solar field based on flat-plate collectros," *Solar Energy*, no. 170, pp. 369-378, 2018.

[33] Z. Tian, B. Perers, S. Furbo and J. Fan, "Analysis and validation of a quasi-dynamic model for a solar collector field with flat plate collectors and parabolic trough collectors in series for district heating," *Energy*, no. 142, pp. 130-138, 2018.

[34] M. A. Abdelghani-Idrissi, S. Khalfallaoui, D. Seguin and L. Vernieres-Hassimi, "Solar tracker for enhancement of the thermal efficiency of solar water heating system," *Renewable Energy*, no. 119, pp. 79-94, 2018.

[35] G. Martinez-Rodriguez, A. L. Fuentes-Silva and M. Picon-Nunez, "Solar thermal networks operating with evacuated-tube collectors," *Energy*, no. 146, pp. 26-33, 2018.

[36] D. Beckman, "Flat-Plate Solar Collectors," in *Solar Engineering of Thermal Processes*, USA, John Wiley & Sons, Inc., 1991, pp. 250-326.

[37] U. Eicker, "Solar Thermal Heating," in *Energy Efficient Buildings with Solar and Geothermal Resources*, United Kingdom, John WIley and Sons Ltd, 2014, pp. 205-296.

[38] D. Beckman, "System Thermal Calculations," in *Solar Engineering of Thermal Processes*, USA, John Wiley & Sons, Inc., 1991, pp. 427-452.

[39] D. Beckman, "Energy Storage," in *Solar Engineering of Thermal Processes*, USA, John Wiley & Sons, Inc., 1991, pp. 382-426.

[40] D. Beckman, "Solar Water Heating: Active and Passive," in *Solar Engineering of Thermal Processes*, USA, John Wiley & Sons, Inc., 1991, pp. 487-496.

[41] D. Beckman, "Solar Cooling," in *Solar Engineering of Thermal Processes*, USA, John Wiley & Sons, Inc., 1991, pp. 588-617.

[42] D. Beckman, "Selected Heat Transfer Topics," in *Solar Engineering of Thermal Processes*, USA, John Wiley & Sons, Inc., 1991, pp. 178-181.

[43] J. P. Holman, "Heat Exchangers," in *Heat Transfer: Tenth Edition*, New York, McGraw-Hill Companies, Inc., 2010, pp. 528-555.

[44] Travel Math, "The latitude and longitude of Jackson Mississippi," Travel Math, [Online]. Available: https://www.travelmath.com/cities/Jackson,+MS. [Accessed 30 August 2019].

[45] T. F. J. Irvine and P. E. Liley, Thermodynamic Property Equations for Steam, London: Academic Press, Inc. (London) Ltd., 1984, pp. 21-24.

[46] T. F. J. Irvine and P. E. Liley, "Thermodynamic Property Equations for Steam (Superheated)," in *Steam and Gas Tables with Computer Equations*, London, Academic Press Inc. (London) Ltd., 1984, pp. 51-52.

[47] "Climate Jackson - Mississppi," U.S. Climate Data, 2019. [Online]. Available: https://www.usclimatedata.com/climate/jackson/mississippi/united-states/usms0175/2019/1. [Accessed 8 May 2019].

[48] B. K. Hodge, "Solar Energy Fundamentals," in *Alternative Energy Systems and Applications*, USA, John Wiley & Sons, Inc., 2010, pp. 114-148.

[49] U.S. Secretary of Commerce, "Propylene Glycol," National Institute of Standards and Technology, 2018. [Online]. Available: https://webbook.nist.gov/cgi/cbook.cgi?ID=C57556&Mask=4. [Accessed 4 December 2019].

[50] M. Souliotis, N. Arnaoutakis, G. Panaras, A. Kavga and S. Papaefthimiou, "Experimental study and Life Cycle Assessment (LCA) of Hybrid Photovoltaic/Thermal (PV/T) solar systems for domestic applications," *Renewable Energy,* no. 126, pp. 708-723, 2018.

[51] H. Cherif, G. Champenois and J. Belhadj, "Environmental life cylce analysis of a water pumping and deslination process powered by intermittent renewable energy sources," *Renewable and Sustainable Energy Reviews,* no. 59, pp. 1504-1513, 2016.

[52] S. Chen, "Life Cycle Assessment of Wood Pellet," Chalmers University of Technology, Goteborg, 2009.

[53] B. Morrison and J. S. Golden, "Life Cycle Assessment of co-firing coal and wood pellets in the Southeastern United States," *Journal of Cleaner Production,* no. 150, pp. 188-196, 2017.

[54] F. Ardente, G. Beccali, M. Cellura and V. L. Brano, "Life cycle assessment of a solar thermal collector," *Renewable Energy,* no. 30, pp. 1031-1054, 2005.

[55] P. L. Spath, M. K. Mann and D. R. Kerr, "Life Cycle Assessment of Coal-fired Power Production," National Renewable Energy Laboratory, Golden, 1999.

[56] M. Ozturk, N. Ozek, H. Batur and M. Koc, "Thermodynamic and life cycle assessment of flat-plate collector, photovoltaic system and photovoltaic thermal collector," *International Journal of Exergy,* vol. 11, no. 2, pp. 229-251, 2012.

VITA

Education and Honor Societies

University of Mississippi University, MS — August 2013 - May 2017
Bachelor of Science in Mechanical Engineering
- GPA: 3.71/4.00 Cum Laude

Golden Key International Honour Society University, MS — December 2016 - Present
Tau Beta Pi, Engineering Honor Society University, MS — October 2016 - Present
National Society of Collegiate Scholars University, MS — August 2014 - Present

Work and Research Experience

Oak Ridge National Laboratory, Manufacturing Demonstration Facility Oakridge, TN — Summer 2019
Graduate HERE Fellowship under Mark Noakes and Andrzej Nycz — Summer 2018
- Worked with Metal Big Area Additive Manufacturing team using stainless and mild steel
- Designed compression molds and a quick change fixture for IMTS 2018 – Chicago
- Piloted 6+3 external axis ABB Robotic Arm – IRB 4600 40/2.55
- Created infill patterns for experimental weld-path geometries
- Produced engineering drawings of parts and systems
- Designed multi-material, printed stamping die for Whirlpool
- Performed 3-D scans of parts using FARO scanner
- Improved design of robot locating mount to reduce vibration
- Fabricated protective cases for welding and infrared camera
- Implemented modeling and finite element software to enhance design of manufactured pieces
- Designed and tested experimental argon enclosure and local shielding gas device

Smith & Nephew Memphis, TN — June 2017 - August 2017
Laboratory Assistant
- Cycled baskets of laser marked medical instruments through autoclave, ultrasonic bath, and washer
- Observed and logged part degradation over the span of long term wear through harsh testing
- Improved the takt time of the testing process by 12%, allowing for an increase of 2 cycles a day

National Center for Physical Acoustics University, MS — Summer 2016
Student Researcher in the BASS Fellowship under Dr. Gautam Priyadarshan
- Gained a working knowledge of electrochemistry and the electrolytic cell
- Gathered information about the application and effects of the introduction of ultrasonic waves into viscous fluids
- Delved into diffusion mechanics and ion transfer of ions in solution to a conductive substrate
- Compiled, presented, and defended findings on of the use of ultrasonication in electroplating